

United Arab Emirates University

Scholarworks@UAEU

Theses

Electronic Theses and Dissertations

1-2024

DEVELOPMENT OF $\text{TiO}_2/\text{NH}_2\text{-MIL-125}$ NANOCOMPOSITE FOR THE REMOVAL OF CIPROFLOXACIN UNDER INDUCED SOLAR IRRADIATION

Bilkis Mojisola Ajiwokewu

Follow this and additional works at: https://scholarworks.uaeu.ac.ae/all_theses



Part of the [Petroleum Engineering Commons](#)

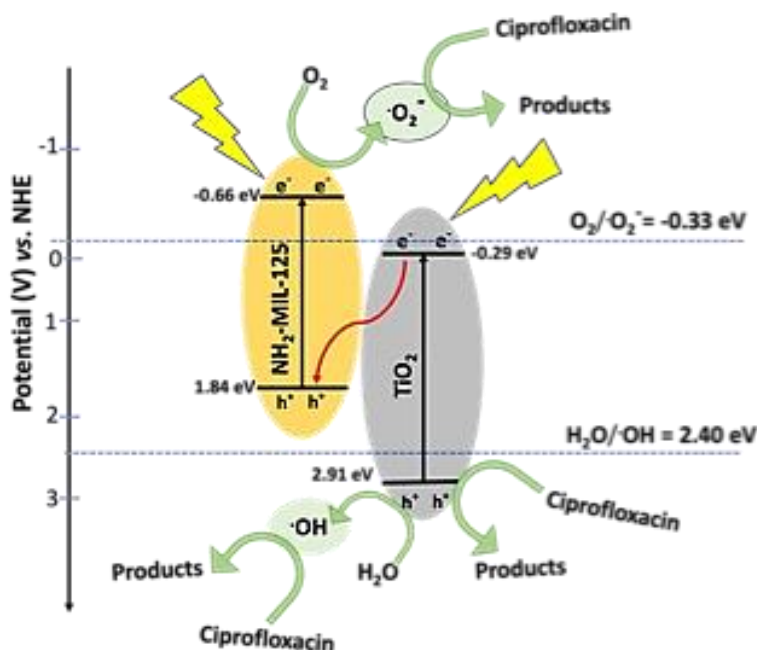
MASTER THESIS NO. 2024: 12

College of Engineering

Department of Chemical and Petroleum Engineering

DEVELOPMENT OF $\text{TiO}_2/\text{NH}_2\text{-MIL-125}$ NANOCOMPOSITE FOR THE REMOVAL OF CIPROFLOXACIN UNDER INDUCED SOLAR IRRADIATION

Bilkis Mojisola Ajiwokewu



January 2024

United Arab Emirates University

College of Engineering

Department of Chemical & Petroleum Engineering

DEVELOPMENT OF TiO_2/NH_2 -MIL-125 NANOCOMPOSITE
FOR THE REMOVAL OF CIPROFLOXACIN UNDER INDUCED
SOLAR IRRADIATION

Bilkis Mojisola Ajiwokewu

This thesis is submitted in partial fulfilment of the requirements for the degree of
Master of Science in Chemical Engineering

January 2024

United Arab Emirates University Master Thesis
2024: 12

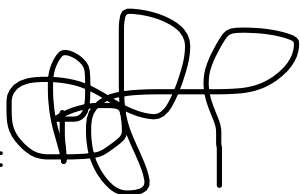
Cover: Z-Scheme heterojunction representing electron transfer
(Photo: By Bilkis Mojisola Ajiwokewu)

© 2024 Bilkis Mojisola Ajiwokewu, Al Ain, UAE
All Rights Reserved
Print: University Print Service, UAEU 2024

Declaration of Original Work

I, Bilkis Mojisola Ajiwokewu, the undersigned, a graduate student at United Arab Emirates University (UAEU), and author of his thesis entitled “*Development of $\text{TiO}_2/\text{NH}_2\text{-MIL-125}$ Nanocomposite for the Removal of Ciprofloxacin under Induced Solar Irradiation*”, hereby, solemnly declare that this is the original research work done by me under the supervision of Dr Mohammad Tahir, in the College of Engineering at UAEU. This work has not previously formed the basis for the award of any academic degree, diploma or similar title at this or any other university. Any materials borrowed from other sources (whether published or unpublished) and relied upon or included in my thesis have been properly cited and acknowledged in accordance with appropriate academic conventions. I further declare that there is no potential conflict of interest with respect to the research, data collection, authorship, presentation and/or publication of this thesis.

Student's Signature:



Date: April 11, 2024


Approval of the Master Thesis

This Master Thesis is approved by the following Examining Committee Members:

- 1) Advisor (Committee Chair): Dr Mohammad Tahir
Title: Assistant Professor
Department of Chemical and Petroleum Engineering
College of Engineering

Signature  Date 18 March 2024

- 2) Member: Dr Mohammednoor Altarawneh
Title: Professor
Department of Chemical and Petroleum Engineering
College of Engineering

Signature  Date 19/3/2024

- 3) Member (External Examiner): Dr Wey Yang Teoh
Title: Associate Professor
Department of Chemical Engineering
Institution: Universiti Malaya, Hong Kong

Signature  Date 19/3/2024

Mohammednoor Altarawneh on behalf of the external examiner

This Master Thesis is accepted by:

Dean of the College of Engineering: Professor Mohamed H. Al-Marzouqi

Signature Mohamed AlMarzouqi

Date May 20, 2024

Dean of the College of Graduate Studies: Professor Ali Al-Marzouqi

Signature Ali Hassan

Date 23/05/2024

Abstract

This research focuses on the development and application of Metal-Organic Frameworks (MOFs)-based nanocomposites for the photocatalytic removal of pharmaceutical contaminants, with a specific emphasis on ciprofloxacin (CIP). The photocatalytic degradation of CIP was investigated using as-synthesized photocatalysts of TiO₂ nanowires (TiO₂NWs), bare MOF of NH₂-MIL-125, TiO₂NW/NH₂-MIL-125 composite, and Lanthanum (La)-doped composite. Intriguingly, the TiO₂NW/NH₂-MIL-125 composite exhibited the highest efficiency, achieving a photodegradation rate of 0.0111 min⁻¹, surpassing the independent performances of bare MOF of NH₂-MIL-125 and TiO₂NW. The observed efficiency was attributed to the formation of a Z-scheme heterojunction which improves charge separation and the generation of active species ($\bullet\text{O}_2^-$ and $\bullet\text{OH}$) under the induced solar irradiation. Furthermore, the first-order rate constant of 0.0111 min⁻¹ estimated for the TiO₂NW/NH₂-MIL-125 photocatalyst demonstrates promising and competitive performance when compared to prior research. This study emphasizes the potential for enhancing MOF photocatalytic properties through formation of heterojunction with inorganic photocatalysts like TiO₂, particularly for pharmaceutical wastewater treatment. This research presents a promising solution for addressing pharmaceutical contaminations and invites further exploration into MOFs-based photocatalysis, recognizing experimental limitations and the scarcity of relevant literature.

Keywords: Photocatalysis, Metal-Organic Framework (MOF), Pharmaceutical contaminants, Ciprofloxacin (CIP), Heterojunction, Lanthanum doping, Z-Scheme, Contaminants of emerging concerns (CECs).

Title and Abstract (in Arabic)

تطوير مركب $\text{TiO}_2/\text{NH}_2\text{-MIL-125}$ لإزالة السيبروفلوكساسين تحت الإشعاع الشمسي المستحث

الملخص

يركز هذا البحث على تطوير وتطبيق المركبات النانوية المكونة من الهياكل الفلزية العضوية (MOFs) لإزالة الملوثات الدوائية عن طريق التحفيز الضوئي، مع التركيز بشكل خاص على السيبروفلوكساسين (CIP). تمت دراسة تحليل CIP عن طريق التحفيز الضوئي باستخدام محفزات ضوئية مُصنَّعة من أسلاك النانوية TiO_2 (TiO_2NWs)، و MOF المجرد المصنوع من $\text{NH}_2\text{-MIL-125}$ ، و المركب $\text{TiO}_2\text{NW}/\text{NH}_2\text{-MIL-125}$ ، ومركب المنشط باللانثانم (La)-doped. من المثير للاهتمام أن المركب $\text{TiO}_2\text{NW}/\text{NH}_2\text{-MIL-125}$ أظهر أعلى كفاءة، حيث حقق معدل تحليل ضوئي قدره 52.4%، متجاوزاً الأداء المستقل لكل من الهياكل الفلزية العضوية المجردة المكونة من $\text{NH}_2\text{-MIL-125}$ و TiO_2NW . تُعزى الكفاءة الملحوظة إلى تكوين وصلة متغايرة على شكل مخطط Z الذي يعمل على تحسين فصل الشحنات وتوليد الأنواع النشطة ($\bullet\text{O}_2^-$ and $\bullet\text{OH}$) تحت الإشعاع الشمسي المستحث. علاوة على ذلك، فإن ثابت معدل الدرجة الأولى البالغ 0.0111 د-1 المقدر للمحفز الضوئي $\text{TiO}_2\text{NW}/\text{NH}_2\text{-MIL-125}$ يُظهر أداءً واعدًا وتنافسيًا عند مقارنته بالبحث السابق. تؤكد هذه الدراسة على إمكانية تعزيز خصائص التحفيز الضوئي للهياكل الفلزية العضوية من خلال تكوين الترابط غير المتجانس مع المحفزات الضوئية غير العضوية مثل TiO_2 ، خاصة لمعالجة مياه معامل الأدوية. يقدم هذا البحث حلاً واعدًا لمعالجة التلوث الناتج عن معامل الأدوية ويدعو إلى مزيد من الاستكشاف الحفز الضوئي القائم على الهياكل الفلزية العضوية، مع ادراك القيود التجريبية وندرة المنشورات العلمية ذات الصلة.

مفاهيم البحث الرئيسية: التحفيز الضوئي، الهيكل الفلزي العضوي (MOF)، الملوثات الدوائية، سيبروفلوكساسين (CIP)، الترابط المتغاير، منشطات اللانثانم، مخطط Z، الملوثات ذات الاهتمامات الناشئة (CECs).

Acknowledgements

I am deeply grateful to Almighty Allah for granting me the strength and grace to successfully complete my master's degree.

I would like to extend my heartfelt appreciation to the Photocatalysis research team of the Department of Chemical & Petroleum Engineering for their unwavering guidance, support, and assistance throughout my thesis research. I want to express special gratitude to my advisor, Dr. Mohammad Tahir, for accepting and supporting my research.

I offer my sincere thanks to my husband, Dr. Ahmed Yusuf (PhD Chemical Engineering), for his unending financial, emotional, and academic support during the entire duration of this program.

I am also immensely thankful for the support I received from the Nigerian Students at UAEU, particularly Dr. Toyin Shittu, Muiz Adamson (Ph.D Chemistry, UAEU), and Babatunde Ogunbadejo (PhD Chemical Engineering, UAEU).

To my dear friends, Rukayat Zakari (PhD Chemistry, Khalifa University), and Anifat Adenike Bojesomo Bankole (PhD Chemistry, Khalifa University), I am grateful for your unwavering emotional support, and for generously leveraging your resources at Khalifa University to assist with the analysis of my samples. Your invaluable support during the challenging phases of my research is deeply appreciated.

Dedication

To my beloved husband and children

Table of Contents

Title	i
Declaration of Original Work	iii
Abstract	vi
Title and Abstract (in Arabic)	vii
Acknowledgements	viii
Dedication	ix
Table of Contents	x
List of Tables	xii
List of Figures	xiii
List of Abbreviations	xiv
Chapter 1: Introduction	1
1.1 Overview	1
1.2 Statement of the Problem	2
1.3 Research Objectives	3
1.4 Relevant Literature Review	4
1.4.1 Sources, Dosage, Transport and Fate, and Treatment of PCs in the Environment	4
1.4.2 Heterogeneous Photocatalysis for Pollutant Degradation	12
1.4.3 MOFs as Photocatalysts in Water Treatment	13
1.4.4 Common Synthesis Technique for Photocatalytic MOFs	17
1.4.5 Strategies for Enhancement of MOF-based Materials for HP	18
1.4.6 Recent Developments in the Application of MOF-based Materials for Pollutant Degradation	22
1.4.7 Potential Contributions and Limitations of the Study	24
Chapter 2: Materials and Methods	28
2.1 Materials	28
2.2 Preparation of Photocatalysts	28
2.2.1 Preparation of TiO ₂ Nanowire (NW)	28
2.2.2 Preparation of TiO ₂ (NW)/NH ₂ -MIL-125	28
2.2.3 Preparation of La/TiO ₂ NW/NH ₂ -MIL-125	29
2.3 Characterization of Synthesized Photocatalysts	29

2.4 Photocatalytic Reactivity Test.....	30
Chapter 3: Results and Discussions	32
3.1 Characterization of the Photocatalysts	32
3.1.1 X-ray Diffraction Analysis	32
3.1.2 Scanning Electron Microscopy (SEM) Analysis	33
3.1.3 Fourier Transform Infrared (FTIR) Analysis	34
3.1.4 Textural Characterization and N ₂ Physisorption	35
3.1.5 UV-Vis Spectroscopy and Band Gap Calculation	38
3.1.6 Fluorescence Emission Spectra	39
3.2 Photocatalytic Efficiency Study	41
3.3 Optimization of Selected Parameters	42
3.3.1 Effect of Illumination Configuration.....	43
3.3.2 Effect of Initial Concentration of CIP Solution	45
3.3.3 Effect of Metal Doping	45
3.4 Reaction Kinetics.....	47
3.5 Mechanism of Photodegradation	49
Chapter 4: Conclusions and Outlook	52
References.....	54
List of Publications	70
Appendix.....	71

List of Tables

Table 1: Comparison of different advanced water treatment technologies.....	9
Table 2: Photocatalytic degradation characteristics for PCs in aqueous media by MOF-based photocatalysts.....	26
Table 3: Porous texture, average pore diameter, and volume	38
Table 4: Rate constant values and their R-squared for the tested photocatalysts	48
Table 5: Comparative data for the removal of CIP in water by various photocatalysts	49

List of Figures

Figure 1: Routes of emerging contaminants	6
Figure 2: Routes of pharmaceutical contaminants (PCs).....	8
Figure 3: Heterogeneous photocatalysis for pollutant degradation	13
Figure 4: Schematic showing how MOFs are formed from metal centers and organic linkers (or Ligand).....	15
Figure 5: Photocatalytic mechanism over a photocatalytic MOFs material.....	16
Figure 6: Zn SBU combined with different linkers to produce variety ZIF MOFs	16
Figure 7: Different approaches adopted for the synthesis of MOF-based materials	19
Figure 8: Post-synthetic modification of MR/NH ₂ -MIL-125(Ti) and MR-MIL- 125(Ti).....	19
Figure 9: Different schemes for the photodegradation of pharmaceutical pollutants	24
Figure 10: A systemic demonstration for the synthesis of TiO ₂ /NH ₂ -MIL-125 composite	29
Figure 11: X-ray diffraction patterns of synthesized photocatalysts.....	33
Figure 12: SEM images.....	34
Figure 13: FTIR analysis of synthesized photocatalysts	35
Figure 14: SBET analysis for NH ₂ -MIL-125 and TiO ₂ /NH ₂ -MIL-125 composite	37
Figure 15: UV-VIS DRS spectra and Tauc plots.....	39
Figure 16: Fluorescence emission spectrum of photocatalysts in spectrofluorometer	40
Figure 17: Removal of the CIP pollutant in water.....	42
Figure 18: Internally illuminated photoreactor heating up after 60 min of reaction.	44
Figure 19: Effect of the illumination configuration on CIP photodegradation using NH ₂ -MIL-125	44
Figure 20: Effect of initial CIP concentration using NH ₂ -MIL-125	45
Figure 21: Effect of doping TNHM with Lanthanum metal at 5%, 20%, 30% La composition.	47
Figure 22: Proposed Z-Scheme heterojunction of TiO ₂ /NH ₂ -MIL-125 nanocomposite.....	51

List of Abbreviations

AMR	AntiMicrobial Resistance
AOPs	Advanced Oxidation Processes
APD	Average Pore Diameter
BJH	Barrett-Joyner-Halenda Model
BP	Black Phosphorus
CECs	Contaminants of Emerging Concerns
CIP	Ciprofloxacin
COD	Chemical Oxygen Demand
DMF	DiMethyl Formamide
Eg	Bandgap
FTIR	Fourier Transform Infrared
H2ATA	2-Amino Terephthalic Acid (H2ATA)
HOMO	Highest Occupied Molecular Orbital
HP	Heterogenous photocatalysis
LaTNHM	La/TiO ₂ /NH ₂ -MIL-125
LMCT	Ligand-to-Metal Charge Transfer
LUMO	Lowest Unoccupied Molecular Orbital
MF	MicroFiltration
MIL	Materials from Institute Lavoisier
MOFs	Metal-Organic Frameworks
N-CQD	N-Doped Carbon Quantum Dots
NCs	NanoComposites
NF	NanoFiltration
NHM	NH ₂ -MIL-125

NW	Nanowire
PCs	Pharmaceutical Contaminants
pH	Potential of Hydrogen
PPCPs	Personal Care Products and Pharmaceuticals
PSE&I	Post-Synthetic Elimination and Installation
PSM	Post-Synthesis Modification
PSME	Post-Synthetic Metal Exchange
RO	Reverse Osmosis
ROS	Reactive Oxygen Species
SBET	Specific surface Area
SBU _s	Secondary Building Units
SEM	Scanning Electron Microscopy
TNHM	TiO ₂ /NH ₂ -MIL-125
TOC	Total Organic Carbon
TPV	Total Pore Volume
TTIP	Titanium Tetra Iso Propoxide
UiO	University of Oslo
WWTPs	Wastewater Treatment Plants
XRD	X-ray Diffraction
ZIF	Zeolitic Imidazolate Frameworks
HRTEM	High-resolution transmission electron microscopy

Chapter 1: Introduction

1.1 Overview

Conventional Wastewater treatment plants (WWTPs) have been widely adopted as a breakthrough for the reuse of wastewater, which has been established as a promising solution to the global water scarcity crisis. However, recent research in waterborne diseases has exposed the limitation of this technology in treating contaminants of emerging concerns (CECs) present in the influent of WWTPs. CECs have been identified as endocrine-disruptive chemicals, which include pharmaceuticals and personal care products, organic pollutants, and heavy metals. Most of which entered the environment through domestic, agricultural, and industrial wastewater runoff. Pharmaceutical contaminants have been detected in various wastewater sources including urban wastewater either in the form of parent compounds or metabolites. To avoid the escape of these CECs into the environment (or bodies of water), tertiary-stage techniques are being increasingly adopted. Many advanced water treatment technologies have been reported for the removal of CECs in water, they include and are not limited to, adsorption, micro and nanofiltration, membrane bioreactor, advanced oxidation processes (AOPs), integrated and hybrid (Eniola et al., 2022). Adsorption is cheap and easy to implement but it is stymied by the generation of secondary pollution as the CECs will only be transferred from one aqueous to a solid phase, which may eventually find their way into the environment when adsorbents are disposed in landfills (Baskar et al., 2022). Micro and nanofiltration on the other hand are energy-intensive and membrane fouling is a common problem and usually leads to secondary pollution (Jafari et al., 2021). AOPs are processes that use reactive radicals to degrade PCs into less harmful intermediate or when completely mineralized to produce water and carbon dioxide (Kavitha, 2022). While several AOPs have been studied over the years, Heterogenous photocatalysis (HP) is a promising green technology for the complete mineralization of organic pollutants, including pharmaceutical contaminants. For this technology, sunlight energy is harnessed to activate the photocatalyst to initiate redox reactions through the

generation of electrons and holes. Hence, the technology is sustainable, renewable, and cost-effective enough to be adopted easily.

1.2 Statement of the Problem

One of the significant classes of contaminants of emerging concern (CECs) is pharmaceuticals in addition to pesticides, personal care products, and microplastics (Shanableh et al., 2019). Over 200 Pharmaceuticals (including sulfamethazine, ciprofloxacin, ofloxacin, acetaminophen, sulphapyridine, diclofenac, ibuprofen, erythromycin, amoxicillin, and other active pharmaceutical ingredients have been identified in aquatic bodies globally (Kavitha, 2022). In the Middle-Eastern region, wastewater received from domestic, commercial, and industrial sources contains high concentrations of acetaminophen, sulfamethoxazole, and ciprofloxacin (Shanableh et al., 2019). Treated (pharmaceutical) industrial wastewater in China, Korea, and India was reported to have high concentrations (mg/L) of hygromycin, lincomycin, or fluoroquinolone antibiotics (Milaković et al., 2019). These pharmaceutical contaminants (PCs) are persistent and not completely removed by wastewater treatment plants (WWTPs), hence their recent global detection in the effluents of WWTP. They are present in low concentrations in the range of ng/L to ng/mL yet can have adverse effects on the ecosystem (Mackuľak et al., 2019). Their detrimental effect on human health and risk to the ecosystem include but are not limited to disruption of homeostasis, antimicrobial resistance (AMR) (Eniola et al., 2019; Ramírez-Durán et al., 2019), acute toxicity of aquatic organisms resulting in genetic disorder and abnormality in behavior (Afsa et al., 2021; Hontela & Habibi, 2013). Growing resistance to antibiotics has been reported as the cause of millions of deaths every year (Lesho & Laguio-Vila, 2019). It is therefore apparent that the treatment of PCs in wastewater is a global challenge, which requires immediate global attention. There is a dire need for a sustainable, cost-effective, and environmentally friendly treatment technology for the complete removal of pharmaceutical contaminants from the effluent of WWTPs. Photocatalysis has emerged as an environmentally friendly and highly efficient method for degrading emerging pollutants. One commonly employed photocatalyst, titanium dioxide (TiO_2), has demonstrated exceptional

photocatalytic activity under ultraviolet (UV) light in applications such as water treatment. Nonetheless, there has been a growing focus on the development of visible light-driven photocatalysts in recent years to enhance their overall effectiveness. Metal-organic frameworks (MOFs), like MIL-125, are promising due to their organic-inorganic hybrid composition, large surface areas, and active sites. MIL-125, with its adaptable structure, holds potential in photocatalysis, especially in water pollutant photodegradation. Its amine-modified form, NH₂-MIL-125, responds to visible light, making it appealing. This NH₂-MIL-125 can form a heterojunction with TiO₂, creating a more effective photocatalyst by boosting visible light absorption and reducing carrier recombination.

The idea within this thesis is to evaluate the use of metal-organic framework materials NH₂-MIL-125 and its nanocomposite of TiO₂ for the photocatalytic removal of the pharmaceutical compound in wastewater, especially water products from the effluent of wastewater treatment plants, as a simple, cost-effective, and sustainable way to provide tertiary treatment of such contaminated water. The scope of this work encompasses the removal of a fluoroquinolone antibiotic under visible-light irradiation. NH₂-MIL-125 is a MOF material of imidazolate organic ligand, along with their anatase TiO₂ composites was to be synthesized, characterized, and used as photocatalysts. The effect of metal doping using Lanthanum was also investigated.

1.3 Research Objectives

The major aim of this study is to evaluate the use of Metal-organic Frameworks (MOFs)-based nanocomposite for the photocatalytic removal of pharmaceutical contaminants in water. The specific objectives of this study are:

1. To synthesize and characterize MOFs and MOFs-based TiO₂ nanocomposite photocatalysts responsive under visible light irradiation.
2. To investigate the effect of metal doping on the performance of the prepared photocatalysts by varying Lanthanum percent composition.

3. To investigate and optimize the photocatalytic performance of the synthesized nanocomposite photocatalysts on synthesized pharmaceutical wastewater, containing ciprofloxacin, a fluoroquinolone antibiotic under solar light irradiation.
4. To propose a reaction mechanism for the photocatalytic system.

1.4 Relevant Literature Review

The section presents a critical review of the recent literature on the removal of pharmaceuticals from wastewater using photocatalytic MOFs and MOFs/photocatalysts nanocomposite materials. The section begins with a review of common PCs (Pharmaceutical Contaminants) in wastewater including their classification, sources, and their impact on the environment and human health. Followed by the development of strategies for improving MOFs-based photocatalysts for the removal of PCs in water. Then, the state-of-the-art achievements in the use of MOFs were summarized and an outlook for improvement of these materials was presented.

1.4.1 Sources, Dosage, Transport and Fate, and Treatment of PCs in the Environment

PCs can be categorized into various types or groups namely: analgesics and anti-inflammatories, antidepressants, antibiotics, antivirals, anticoagulants, sedatives, cardiovascular, etc. Analgesics and anti-inflammatories are employed commonly to relieve pain and suppress fever. Analgesics are the main source of PCs into wastewater (Batt et al., 2007). Diclofenac, ibuprofen, paracetamol, etc. are common over the counter anti-inflammatory and analgesic medications (Jiménez-Bambague et al., 2020; Kumar et al., 2019; Kumar et al., 2022). Antibiotics are toxic to microbes and prevent the development of bacteria in the body (Mamta et al., 2020). Antibiotics destroy and suppress the development of microorganisms in wastewater, which affects the treatment process in WWTPs that rely on microbial activity (Tiwari et al., 2017). Antibiotics consist of diverse compounds with various functional groups that influence a wide range of physical and chemical properties, as well as their behavior within ecosystems. These compounds are considered persistent or pseudo-persistent because they enter the environment at a faster rate than they are eliminated from it.

Antibiotics can be categorized into different groups based on their mode of action and chemical composition. Antibiotics within the same structural class tend to exhibit similar efficacy, toxicity, and allergic reactions. As a result, the following types of antibiotics have been studied: beta-lactams, macrolides, tetracyclines, quinolones, aminoglycosides, sulphonamides, glycopeptides, and oxazolidinones (Nkoh et al., 2023). Antidepressants are neuroactive drugs used to manage addictions, cure chronic pain issues, and treat depression as well as anxiety (Mamta et al., 2020). Lajeunesse (2012) and Metcalfe et al. (2010) discovered that antidepressants and their metabolites can be found in sewage, surface water, and even the discharge of wastewater treatment facilities. Fluoxetine, lipid-lowering medications, antacids, ciprofloxacin, diclofenac, steroids, beta-blockers, clofibrilic acid, analgesics, antipyretics, antibiotics, anti-inflammatory drugs, stimulants, salicylic acid, antidepressants, nitroglycerin, and propranolol are the pharmaceuticals that are most detected in drinking water and wastewater (Benotti et al., 2009).

The most common ways that PCs get into the environment are through human waste disposal, the discarding of unwanted medicines, pharmaceutical use in agriculture, Sewage treatment plants (STPs), WWTPs, sanitary landfill leaching, etc. (Le et al., 2021; Naushad et al., 2019; Stuart et al., 2012; Tran et al., 2014). Figure 1 is the illustrative representation of common sources and routes of CECs (Rathi et al., 2021). According to Rozman et al. (2017) and Shraim et al. (2017), pharmaceuticals are typically present in water at low concentrations and can be found in ng/mL and ng/L in water samples taken before and after municipal wastewater treatment and sewage plant treatment, respectively.

In Slovakia, traces of diclofenac (110 ng/L), carbamazepine (340 ng/L), metoprolol acid (430 ng/L), and sulfamethoxazole (240 ng/L) were detected in surface waters. Some of these medications can have a negative impact on the ecosystem even at low environmental concentrations of 1-500 ng/L (Mackuľak et al., 2019). There are several worldwide reports of PC releases into the environment. For instance, 93 pharmaceuticals were discovered in surface water in the United States (Deo, 2014). In a study conducted in China by Zhang et al. (2015), 53,800 tons of pharmaceutical

chemicals (out of 54000 tons excreted by humans and animals) were released into the environment after treatment.



Figure 1: Routes of emerging contaminants (Rathi et al., 2021)

In a study carried out by Shanableh et al. (2019) at the Sharjah wastewater treatment plant (WWTP), 10 pharmaceuticals were detected in a total of 224 wastewater effluent, seawater, and sediment samples collected from December 2021 to October 2022. The wastewater effluent samples were collected from the effluent pipe ends at the central Sharjah WWTP while Seawater and sediment samples were gathered along the Sharjah coastline extending from Al Heera Beach to Al Khan Beach. The maximum removal efficiencies reported are sulfapyridine (73%), sulfamethoxazole (65%), sulfadiazine (52%), ofloxacin (49%), ciprofloxacin (46%), erythromycin (39%), risperidone (95%), metoprolol (39%), and acetaminophen (97%). The physiochemical nature of pharmaceuticals also influences their removal rates. For example, acetaminophen undergoes degradation during conventional treatment while risperidone is susceptible to adsorption onto particles. This explains its high removal rate in this study. On the other hand, antibiotics are more resistant to biodegradation and selective in adsorption behavior (Nkoh et al., 2023). Interestingly,

ciprofloxacin and sulfamethoxazole levels are comparable to earlier studies in Saudi Arabia, a neighboring country to the UAE. Al Qarni et al. (2016) reported a high level of ciprofloxacin in the influent of hospital wastewater at a concentration of up to 5611 ng/L while Alidina et al. (2014) had earlier reported a high concentration of 730 ng/L in the effluent of municipal wastewater. In a more recent study on the assessment of 16 selected pharmaceuticals in Riyadh wastewater treatment plants, ciprofloxacin, and ofloxacin posed the highest environmental risk (Alharbi et al., 2023). Ciprofloxacin appears to be a commonly detected PC in wastewater in the Gulf region. Moreover, Nas et al. (2021) claim that ciprofloxacin and sulfamethoxazole are two widely consumed antibiotics from the fluoroquinolone and sulfonamide groups, respectively.

Pharmaceutical pollutants in the environment are believed to come from both personal care products and pharmaceuticals (Figure 2) (Samal et al., 2022). Depending on their physicochemical characteristics, PPCPs can be found in the aquatic environment, soil, and even in the food chain by uptake from animals or plants. PPCPs can leach into the groundwater via fertilizer used to fortify the productivity of agricultural produce. Food crops can absorb PPCPs as nutrients, which could be dangerous for human consumption. PCs change into stable molecules that are naturally safe through a variety of physiochemical and biological mechanisms. The PCs can also go through mineralization, degradation, or slight structural changes during degradation. According to Kagle et al. (2009), the mineralization of PCs is the process by which these pollutants are converted into carbon dioxide, water, and inorganic ions. PCs break down into smaller chain products or compounds during the process of degradation lowering their quantities in the environment (Blair et al., 2013). However, when these substances are transformed into newer, lower-molecular-weight substances (degraded by-products or metabolites), they can be more harmful to aquatic life than the parent substance. According to Chiron et al. (2006), solar light intensity, light penetration, organic matter, latitude, seasonality, salinity, dissolved solids, PPCP concentration, etc. all affect how much photodegradation occurs in aquatic conditions.

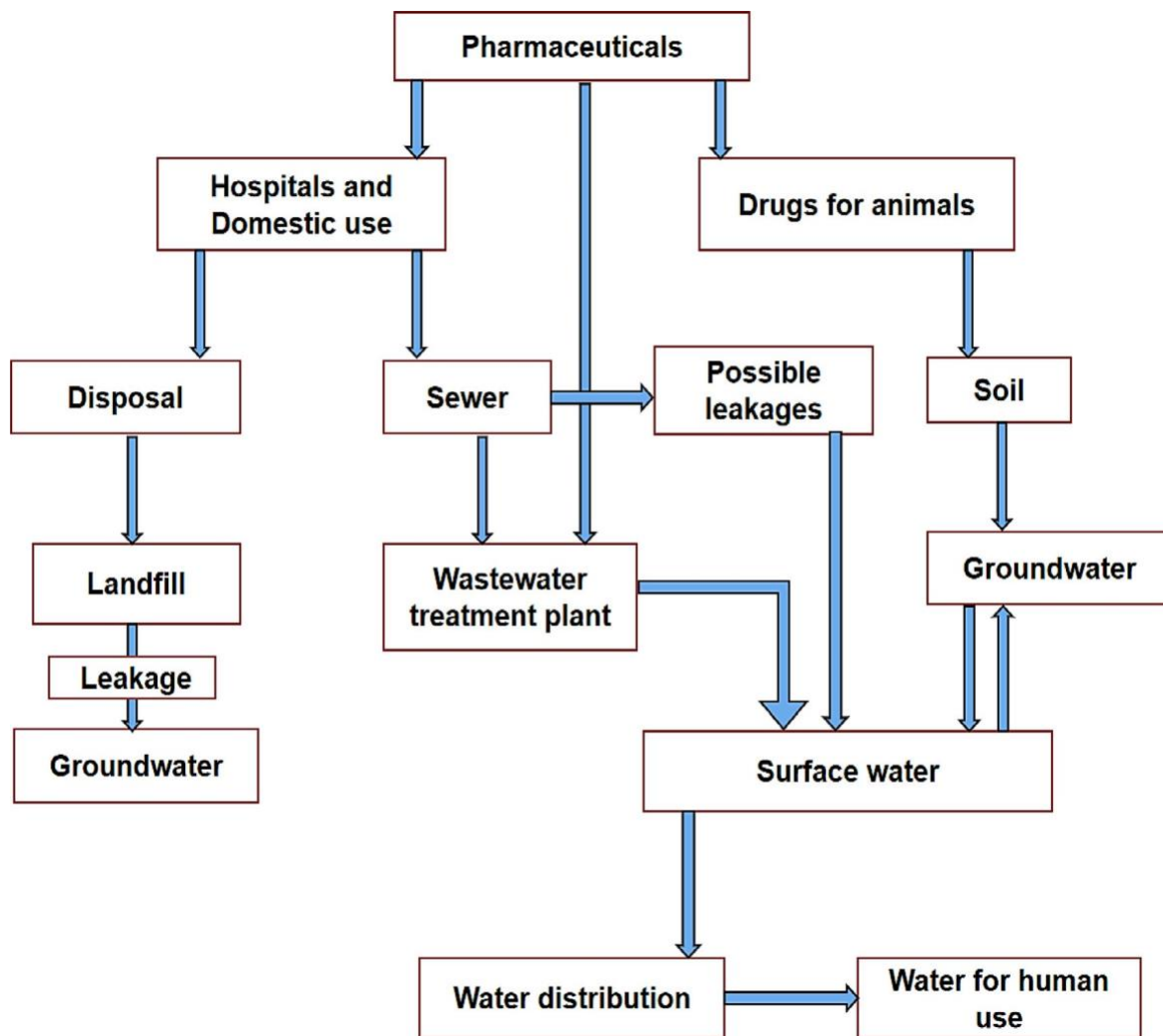


Figure 2: Routes of pharmaceutical contaminants (PCs) (Samal et al., 2022)

Table 1: Comparison of different advanced water treatment technologies

Treatment Technology	Advantages	Disadvantages
Aerobic and anaerobic treatment	<ul style="list-style-type: none"> • Combined aerobic and anaerobic treatment systems offer a more competent bioremediation method for PCs in wastewater (Shah & Shah, 2020). • Anaerobic treatment offers reduced sludge output and low operation costs. (Zhou et al., 2006) 	<ul style="list-style-type: none"> • High energy-consuming processes (Skouteris et al., 2020) • Aerobic is less effective for high-strength pharmaceutical wastewater (Phoon et al., 2020)
Photocatalysis	<ul style="list-style-type: none"> • Can mineralize recalcitrant organic pollutants like PCs without producing harmful byproducts. • Offers high degradation efficiency for pharmaceutical wastewater treatment. • Offers versatility in treating both biodegradable and non-biodegradable compounds and it is applicable to a wide range of pharmaceuticals and intermediates. 	<ul style="list-style-type: none"> • Ineffective for the treatment of pharmaceutical compounds that are resistant to degradation. • It's stymied by limited light spectrum absorption (just about 4% of the solar spectrum). • Electron-hole recombination leads to low efficiency. • Catalyst regeneration and recovery might be time-consuming and have cost implications.

Table 1: Comparison of Different Water Treatment Technologies (Continued)

Treatment Technology	Advantages	Disadvantages
Photocatalysis	<ul style="list-style-type: none"> • With the use of UV, visible light, solar light, and a photocatalyst like TiO₂, ZnO, or CdS, it is environmentally friendly. • It is considerably cost-effective and scalable. 	
Adsorption	<ul style="list-style-type: none"> • Low cost • Reusable adsorbents • Ease of operation • Strong binding adsorbents' ability • Natural and agricultural materials have been employed as adsorbents, including zeolites, clay, polymers, graphene, carbon nanotubes, and agricultural waste (de Andrade et al., 2018). 	<ul style="list-style-type: none"> • The efficiency of the adsorbent depends on many parameters including solution pH, time, temperature, surface charge of the material, concentration, and nature of the PC (Eniola et al., 2019).

Table 1: Comparison of Different Water Treatment Technologies (Continued)

Treatment Technology	Advantages	Disadvantages
Membrane filtration technologies	<ul style="list-style-type: none"> • Reverse osmosis (RO), nanofiltration (NF), ultrafiltration, and microfiltration (MF) are a few of the methods used in the membrane process. • RO and NF can yield high-quality effluents (Khanzada et al., 2020). 	<ul style="list-style-type: none"> • RO and NF are energy-intensive, and pressure driven. • Membrane fouling • Low removal efficiency for PCs
Membrane bioreactor	<ul style="list-style-type: none"> • Higher efficiency and better sludge retention. • It has higher biodegradation efficiency. • Low carbon footprint • Low sludge production • It can handle varying pollutant loads. 	<ul style="list-style-type: none"> • Driven mostly by membrane filtration in PC treatment, • PCs are resistant to biological treatments.
Hybrid technologies	<ul style="list-style-type: none"> • The combination of two or more removal techniques results in improved treatment quality. • More effective compared to a single process. 	<ul style="list-style-type: none"> • May be more energy consuming. • May require a budget for pretreatment processing. • Integrated processes may be complex and unyielding and may influence the efficiency of the combined process.

1.4.2 Heterogeneous Photocatalysis for Pollutant Degradation

Photocatalysis is an advanced oxidation process (AOP) technology that uses solar energy to trigger catalytic reactions in normal atmospheric conditions. Unlike traditional catalytic reaction engineering, which relies on thermal energy, photocatalysis harnesses the power of sunlight, a renewable energy source, making it a green technology (Jarusheh et al., 2022; Palmisano et al., 2007; Wankhade et al., 2013). In photocatalysis, the catalyst can either be homogeneous or heterogeneous. The key distinction lies in the phase in which the catalyst operates. In this work, the main interest is in heterogeneous photocatalysis (HP). To effectively trigger oxidation-reduction reactions, HP (heterogeneous photocatalysis) utilizes special semiconductors known as photocatalysts. These photocatalysts harness solar light irradiation from the sun. The photon energy of the light must be equal to or greater than the band gap (E_g) of the photocatalyst for light absorption and the generation of electron-hole ($e^- - h^+$) pairs. This process produces reactive oxygen species (ROS) that are essential for the reactions to occur as shown in Figure 3 (Ren et al., 2021). In the presence of the generated ROS, the photocatalyst surface adsorbs pollutants (such as PCs) present in water. Through an oxidation reaction, these pollutants undergo mineralization into CO_2 , water, and other byproducts. This entire process is enabled by the ability of the photocatalyst to harness solar energy and utilize it effectively in the degradation of pollutants. TiO_2 , ZnO , Fe_2O_3 , C_3N_4 , and bismuth-based materials are commonly used as photocatalysts in water treatment (Majumder et al., 2020; Ren et al., 2021). However, the use of bare photocatalysts has become less popular due to their limited wide bandgap, resulting in poor absorption of visible light and the recombination of electron-hole pairs on the surface (Kavitha, 2022). For example, TiO_2 and ZnO have bandgaps of 3.2 eV and 3.37 eV respectively, making them responsive only to UV light, which represents a small portion of the solar spectrum. This recombination process leads to energy dissipation instead of desired reactions (Ong et al., 2016).

To address the limitations of bare photocatalysts, researchers have developed heterojunction-type photocatalysts. These advanced photocatalysts utilize a

combination of two semiconductors with distinct band structures and electronic properties, working in synergy to enhance the photocatalytic process (Low et al., 2017). While considerable research has focused on inorganic semiconductor heterojunctions, their efficacy in removing organic contaminants remains constrained by inadequate charge carriers responsible for generating ROS, primarily due to high recombination rates and low charge separation efficiency (Fu et al., 2018). Consequently, there is a pressing need for a versatile and adjustable material with the desired characteristics to overcome these limitations and achieve improved photocatalytic performance.

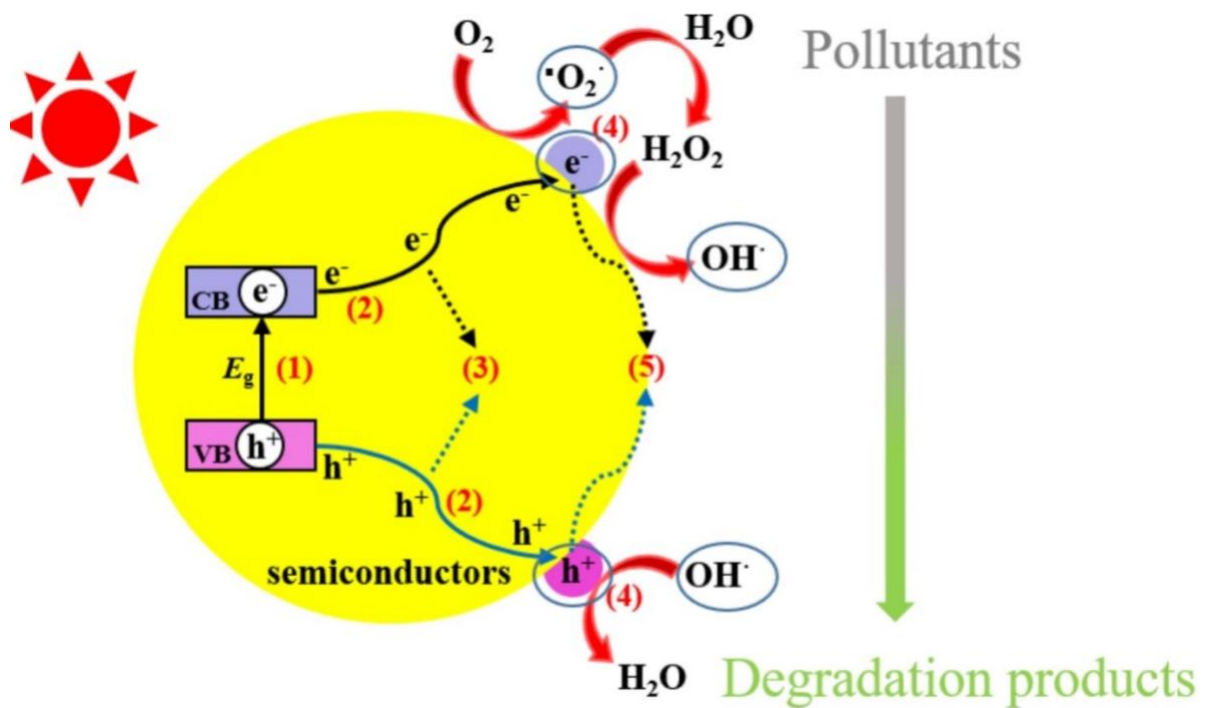


Figure 3: Heterogeneous photocatalysis for pollutant degradation (Ren et al., 2021)

1.4.3 MOFs as Photocatalysts in Water Treatment

With their exceptional properties, metal-organic frameworks (MOFs) have emerged as promising semiconductors for removing pharmaceutical pollutants from water. Metal-organic frameworks (MOFs) are a type of crystalline porous materials formed by connecting metal clusters with organic linkers as shown in Figure 4 (Zhang et al., 2020). These metal clusters, also known as secondary building units (SBUs), play a crucial role in constructing MOFs with high porosity and large surface areas.

The semiconductor-like behavior of MOFs can be attributed to their metal-oxo clusters and organic linkers, acting as isolated quantum dots or light-absorbing antennas (Lv et al., 2021). Unlike traditional inorganic semiconductors like TiO_2 , MOFs exhibit localized conduction and valence bands. Their bandgap energy is determined by the disparity between the energy levels of the highest occupied molecular orbital (HOMO) and the lowest unoccupied molecular orbital (LUMO), corresponding to the valence and conduction bands, respectively (Ikreedeeagh & Tahir, 2021). Most MOFs exhibit photocatalytic behavior attributed to either ligand-to-metal charge transfer (LMCT), metal-to-ligand charge transfer (MLCT), or the $\pi-\pi^*$ transition within organic ligands containing aromatic rings (Zhang & Lin, 2014). A key mechanism driving MOFs' efficacy is the ligand-to-metal charge transfer, where excited electrons transition from the HOMO to the LUMO within the crystalline structure (Figure 5) (Q. Wang et al., 2020). This unique feature amplifies their photocatalytic prowess, enabling the efficient degradation of pharmaceutical pollutants in water. In the degradation of pharmaceuticals in water or wastewater, MOFs play a vital role. When MOFs absorb light, they generate photoelectrons. These photoelectrons can then transfer to oxygen (O_2) and produce superoxide radicals ($\bullet\text{O}_2^-$). Simultaneously, the holes (h^+) in the MOFs' HOMO can oxidize water, generating hydroxyl radicals ($\bullet\text{OH}$). Together, the superoxide and hydroxyl radicals effectively break down and remove pharmaceutical contaminants.

One of the key advantages of MOFs is their ability to undergo various structural transformations by choosing specific central metals and organic linkers. This flexibility allows for the design and synthesis of MOFs with tailored properties and functionalities. For example, different MOFs are produced using the same SBU, but different linkers as shown in Figure 6. The variation in organic linkers influences the pore shapes (Bedia et al., 2019). This highlights the flexibility and tunability of MOFs in terms of their porosity, which can be tailored to suit specific applications or adsorption needs.

MOFs possess a host of advantageous characteristics that make them ideal for heterogeneous photocatalysis. MOFs offer advantages over traditional photocatalytic

semiconductors, with their porous structure enabling efficient diffusion to active sites, high surface area for composites, and adjustable spectral response through functional groups. These characteristics play a crucial role in photocatalysis for degrading organic pollutants (Xia et al., 2021). Although their application for water treatment is challenged by their chemical stability, MOFs classified as MIL (Materials from Institute Lavoisier), UiO-66 (University of Oslo), and Zeolitic imidazolate frameworks (ZIF) are stable MOFs due to the strength of metal-ligand bonds (Wen et al., 2021).

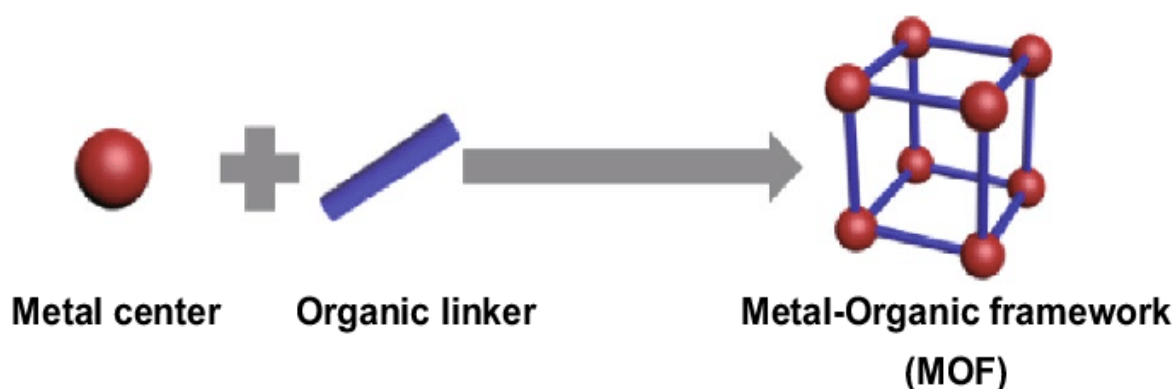


Figure 4: Schematic showing how MOFs are formed from metal centers and organic linkers (or Ligand) (Zhang et al., 2020)

Another limitation of pure forms of many metal-organic frameworks (MOFs) is visible light absorption. To overcome these hurdles, various strategies have emerged to enhance MOFs for pharmaceutical degradation. MOFs possess a tunable structure, allowing for band gap engineering through doping and heterojunction formation, as well as morphological alterations like metallic nanoparticles (Tahir et al., 2023; C. C. Wang et al., 2020). Functionalization with amine reagents, Fenton reagents, and plasmonic reagents has also shown promise (Swetha et al., 2022). These modifications improve stability and boost MOFs' responsiveness to visible light. With their large surface area, active sites, photo-responsiveness, and chemical stability, MOFs offer optimal conditions for efficiently degrading pharmaceutical pollutants (Wen et al., 2021).

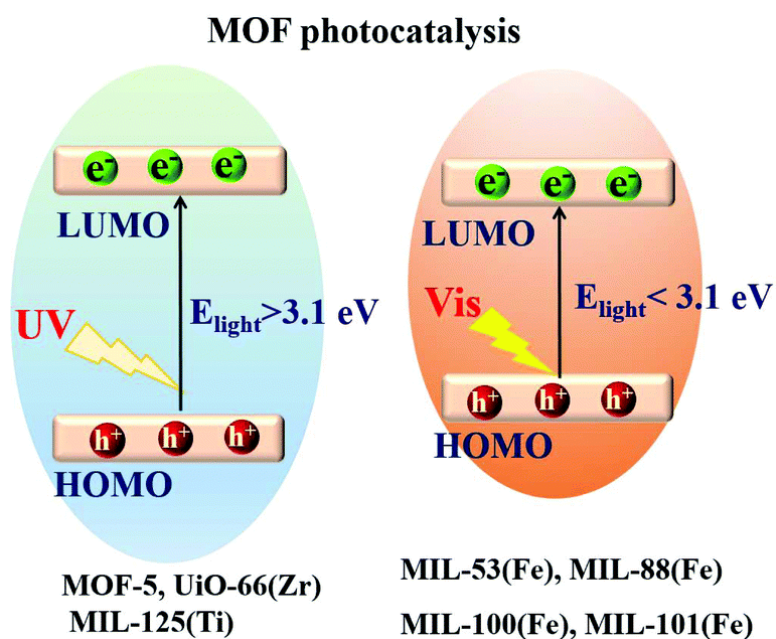


Figure 5: Photocatalytic mechanism over a photocatalytic MOFs material (Wang et al., 2020)

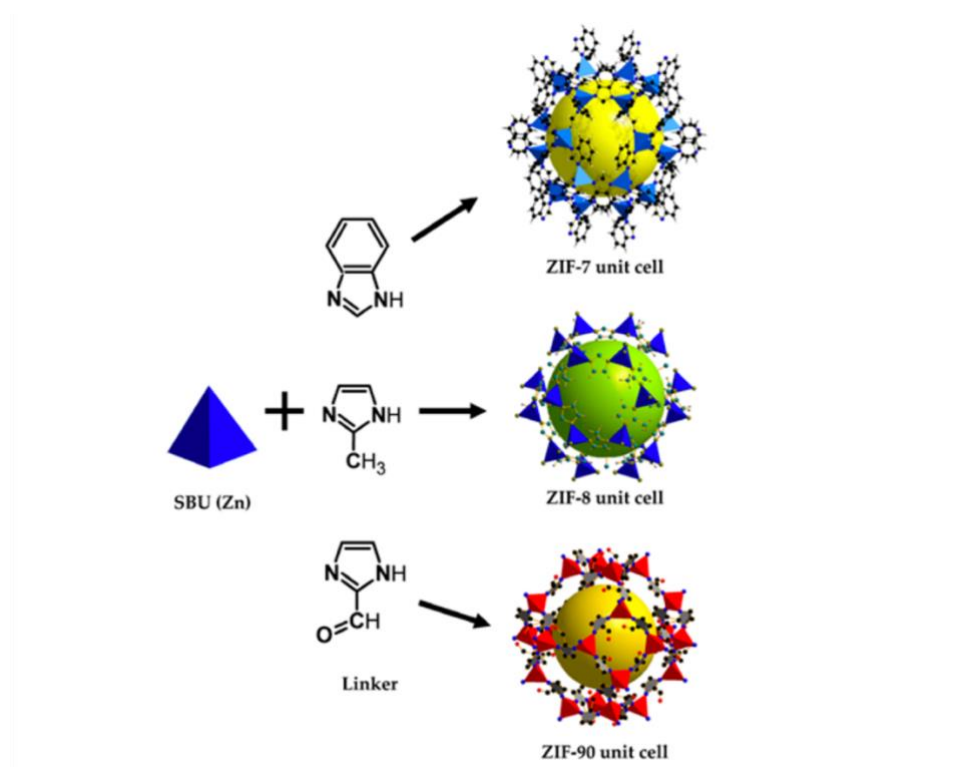


Figure 6: Zn SBU combined with different linkers to produce variety ZIF MOFs (Bedia et al., 2019)

1.4.4 Common Synthesis Technique for Photocatalytic MOFs

MOFs are commonly synthesized using liquid-phase methods, which involve mixing metal and ligand precursors or adding a solvent to a mixture of metal salt and ligand. The choice of solvent is influenced by factors such as solubility, reactivity, stability constant, and redox potential. Several synthetic approaches have been developed for MOF preparation, including solvothermal synthesis, sonochemical methods, microwave synthesis, mechanochemical methods, electrochemical procedures, and slow evaporation. The pictorial illustration shown as Figure 7 summarizes the synthesis approaches discussed below (Ikreedeeh & Tahir, 2021).

Solvothermal synthesis (Nunes et al., 2019) is a highly efficient strategy that allows for precise control over shape and size distribution, with the added benefits of high yield, easy operation, and low temperature and pressure conditions. Microwave-assisted method (Krishnan et al., 2022), on the other hand, offer significantly faster synthesis rates compared to traditional heating techniques. By heating the solution using microwaves, the reaction time is reduced, resulting in high efficiency, particle size reduction, and improved morphology control. Mechanochemical synthesis (Dubadi et al., 2023) represents a solvent-free approach to MOF fabrication. This method involves applying mechanical force to induce a chemical reaction, which can occur in either a steady-state manner or a self-propagating combusive manner. One of the major advantages of this method is that it eliminates the use of organic solvents, which can have detrimental effects on the environment (Mumtaz et al., 2022). Sonochemical methods (Qi et al., 2022) utilize ultrasound waves to promote homogenous nucleation and significantly reduce crystallization time compared to conventional methods. Electrochemical procedures (Barzegar et al., 2019) enable metal salt-free synthesis by introducing metal ions via anodic dissolution into a synthetic mixture containing electrolyte and organic linkers. Slow evaporation (Raptopoulou, 2021) is a simple and convenient method for MOF synthesis, as it does not require an external energy source and can be carried out at room temperature. However, it is a time-consuming process that can be mitigated by using solvents with low boiling points. It is worth noting that the synthesis of nano-MOFs and the

production of monodisperse and uniform nano-MOF particles remain challenging tasks. Further research and development are needed to overcome these challenges and improve the synthesis techniques, particularly at the nanoscale. Notwithstanding, different synthetic methods offer distinct advantages and limitations for MOF synthesis. Researchers continue to explore and refine these methods to enhance the synthesis of MOFs and address the challenges associated with nano-MOF production.

1.4.5 Strategies for Enhancement of MOF-based Materials for HP

A. Post-synthesis modification (PSM)

PSM is the key to unlocking the full potential of MOFs and it involves modifying the MOF structure and properties after synthesis, enabling the introduction of functional groups and customization of surfaces. PSM empowers researchers to fine-tune MOFs for specific applications, boosting catalytic activity, selectivity, and stability. Techniques like post-synthetic metal exchange (PSME) and post-synthetic elimination and installation (PSE&I) offer precise modifications, elevating MOFs' photocatalytic performance. With PSM, MOFs become highly adaptable and optimized materials, maximizing their efficiency in various catalytic processes. PSM is the key that unlocks the full potential of MOFs, transforming them into powerful tools for advanced applications in the field of materials science and catalysis. Figure 8 shows an example from the work of Fu et al. (2021) where partial PSM of MR/NH₂-MIL-125(Ti) was achieved by replacing some NH₂ groups with MR chromophores.

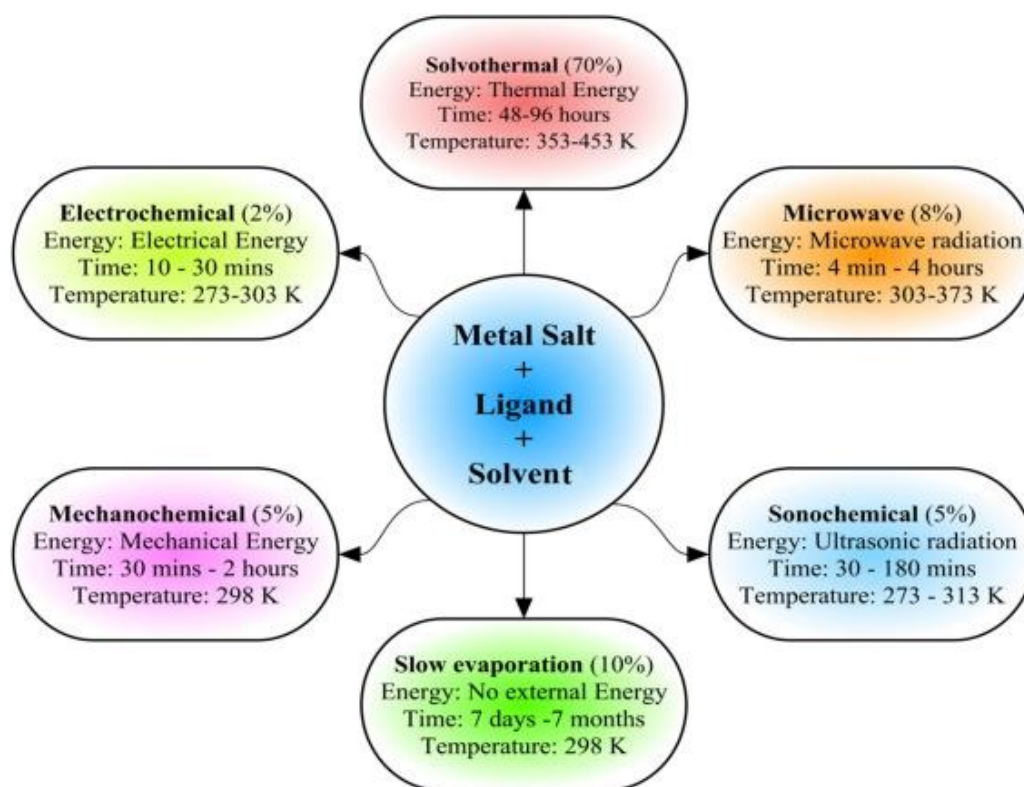


Figure 7: Different approaches adopted for the synthesis of MOF-based materials (Ikreedeegh & Tahir, 2021)

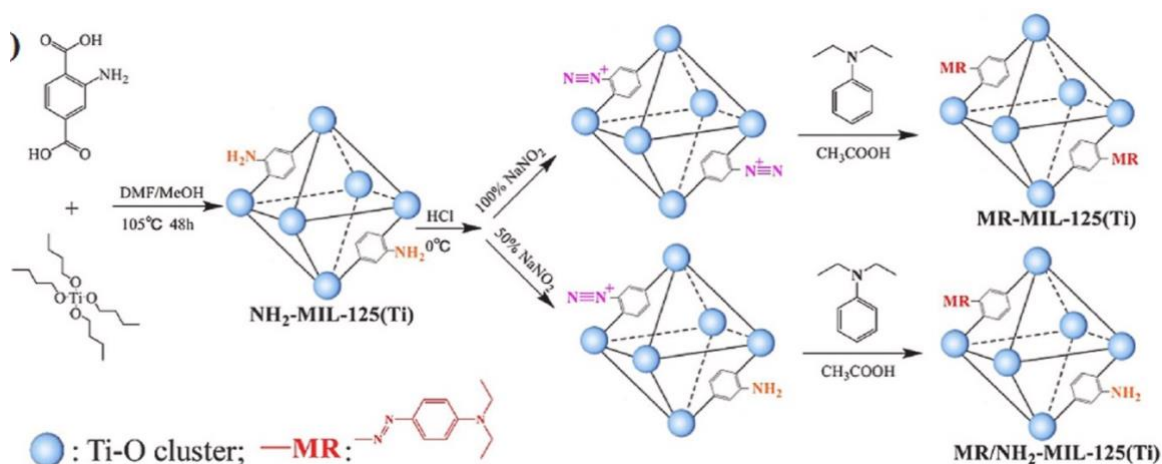


Figure 8: Post-synthetic modification of MR/NH₂-MIL-125(Ti) and MR-MIL-125(Ti) (Fu et al., 2021)

B. Functionalization with ligands and substituents

This strategy involves the deliberate modification of MOFs by introducing specific functional groups or substituents into the structure of the ligands. This process enables researchers to tailor the properties and performance of MOFs for various applications. Ligand functionalization involves attaching additional chemical groups to the ligands, which are the organic molecules that bind to the metal ions in MOFs. By introducing functional groups, such as amino, carboxylate, or hydroxyl groups, the chemical reactivity, selectivity, and stability of the MOFs can be altered. This allows for the customization of both the interior and exterior surfaces of the MOFs, enhancing their catalytic activity and adsorption capabilities. Similarly, substituents are chemical groups or atoms that replace existing groups within the ligand structure. These substitutions can have a significant impact on the properties of the MOFs. For example, the band gap of NH₂-MIL-125 is lower compared to pristine MIL-125 due to the amine functional group present in NH₂-MIL-125. This decrease in band gap extends the optical absorption from 350 to 550 nm, improving the MOF responsiveness to visible light (AbdulMubarak et al., 2022). The discovery of functionalization of MIL-125 to NH₂-MIL-125 has made the latter attractive for photodegradation of pharmaceuticals. More active sites are available that encourage the formation of •OH radicals (AbdulMubarak et al., 2022; Hendon et al., 2013).

C. Introducing dopants and co-catalyst

Elemental doping and co-catalyst incorporation are proven strategies for enhancing the performance of photocatalysts. The versatile nature of MOFs lends itself well to these techniques, strengthening their photocatalytic activity. For example, the introduction of N-doped carbon quantum dots (N-CQD) into MOF-5 resulted in a 2.5-fold increase in the efficiency of photocatalytic Cr (VI) reduction compared to the pure MOF-5. By acting as electron acceptors, N-CQDs improved charge separation during the process (Qin et al., 2021). Another study demonstrated that coupling reduced Ti-based MOFs (BP/R-Ti-MOFs/Pt) with black phosphorus (BP) and a platinum co-catalyst increased photocatalytic hydrogen production by a remarkable 10.3 times compared to pristine Ti-MOFs (Liu et al., 2018). The strong

interaction between BP and Ti on the surface of black phosphorus contributed to this significant enhancement. Furthermore, the incorporation of Ni₃(HITP)₂ MOF nanosheets as a co-catalyst in a hybrid system with [Ru(bpy)₃]²⁺ photosensitizer and TEOA (triethanolamine) electron donor led to an impressive rate of photocatalytic CO₂ reduction, achieving selectivity of 97% and a rate of up to $3.45 \times 10^4 \mu\text{mol g}^{-1} \text{h}^{-1}$ (Zhu et al., 2018). These findings highlight the potential of elemental doping and co-catalyst integration in MOFs to boost the efficiency of photocatalytic reactions.

D. Heterojunction designing and bandgap engineering

Enhancing photocatalysis in MOFs can be achieved through the formation of heterojunctions, which enable band engineering and improve electro-conductivity. When different semiconductors are combined, an electric field is generated due to the disparity in their band potentials, leading to charge separation and electron transfer. This reduces the recombination of photo-induced charges and promotes efficient photocatalysis. MOFs exhibit a wide range of band gaps, typically determined by their metal clusters, organic linkers, and guest compounds. For example, the embedding of Zn_{0.2}Cd_{0.8}S nanoparticles into hydrolyzed MOF-5 nanosheets resulted in improved charge mobility and reduced photo corrosion, achieving a remarkable photocatalytic hydrogen production rate of $15.08 \text{ mmol h}^{-1} \text{g}^{-1}$, 7.62 times higher than pure Zn_{0.2}Cd_{0.8}S (Cui et al., 2020). Additionally, QDs/MOF-based photocatalysts, such as CsPbBr₃ QDs UiO-66(NH₂) nanocomposites (NCs), demonstrated significant visible-light-induced electron exchange at nano-heterojunctions, leading to enhanced photoactivity (Wan et al., 2019). Other strategies include utilizing graphene oxide-based MOFs for synergistic photocatalysis and designing MOF-on-MOF hybrids to exploit their combinational effects. These advancements in heterojunction formation and band engineering offer promising avenues for achieving efficient and selective photocatalytic reactions in MOFs.

E. Modulation of metal-oxidation state

Controlling the metal clusters within MOFs is crucial for optimizing their photocatalytic activity. Gong et al. (2021) successfully enhanced hydrogen production six-fold by oxidizing the metal cluster of Pt/Ce-TTCA (Triphenylene-2,6,10-

tricarboxylic acid), highlighting the importance of regulating the oxidation state. Likewise, Chen et al. (2019) demonstrated that adjusting the Fe^{2+} and Fe^{3+} ratios in mixed-valence MIL-53(Fe) improved photodegradation performance, resulting in maximum degradation rates for different dyes. This manipulation also caused a shift in the bandgap, favoring visible-light catalysis. The impressive outcomes were observed not only in MIL-53(Fe) but also in MIL-88(Fe) and MIL-101(Fe). These findings emphasize the significance of precise control over metal clusters in MOFs, enabling efficient and customizable photocatalytic processes. By fine-tuning the oxidation state and electronic arrangement, researchers can greatly enhance the overall photocatalytic performance of MOFs, opening exciting possibilities for practical applications across various domains.

1.4.6 Recent Developments in the Application of MOF-based Materials for Pollutant Degradation.

The escalating need for efficient and cost-effective wastewater treatment solutions has been spurred by rapid industrialization worldwide. Synthetic dyes, antibiotics, organic pollutants, pharmaceuticals, and heavy metals are among the major water pollutants (Zhang et al., 2021). Photocatalytic degradation, utilizing renewable solar energy, offers a promising approach to completely mineralize these harmful substances. In MOF-based materials, photocatalytic degradation occurs through processes such as ligand-to-metal charge transfer and metal-oxo cluster excitation, leading to the production of reactive oxygen species (ROS). Ligands with filled molecular orbitals or high energy lone pair electrons can absorb light and generate excited electrons that transfer to the metal clusters, facilitating the degradation process. Compared to conventional photocatalysts, MOF-based materials offer superior photocatalytic degradation due to their charge transfer pathways. Real-world studies have demonstrated the effectiveness of MOF-based photocatalysts in treating textile, agrochemical, and pharmaceutical wastewater, achieving significant reductions in chemical oxygen demand (COD) and total organic carbon (TOC). One crucial aspect in these applications is the stability of MOFs in water over extended periods of time and across a wide pH range. The stability of MOFs in aqueous

environments is influenced by factors such as the chemical composition of the MOF, the presence of water molecules in the MOF structure, and the pH of the solution (Bedia et al., 2019; Wen et al., 2021). Ongoing research works have been actively on designing MOFs with enhanced stability in water. Strategies include modifying the ligands or metal nodes used in the MOF synthesis to increase water stability, introducing functional groups that can interact with water molecules, and developing methods to protect the MOF structure from degradation.

Table 2 summarizes recent applications of MOFs-based photocatalysts employed for the degradation of pharmaceutical pollutants in an aqueous medium. MOFs are combined with visible light-driven photocatalysts to improve the degradation efficiency of the composite. In all the studies, the composites have been reported to have improved removal efficiency when compared with individual semiconductors. It can be observed that complex MOF composites have been targeted at antibiotics in aqueous media with a concentration in the average of 10 - 20 ppm, the average catalytic loading observed is 0.2 – 0.5 g. L⁻¹. The average reaction time is between 60 to 120 min under light irradiation. Several possible schemes have been inferred in the studies, which include metal/carbon doping, Type II heterojunction, Z-Schemes, and S-Scheme. In a few cases, MOF materials are employed as sacrificial templates for two other semiconductors forming heterojunctions. Figure 9 shows four different schemes observed in the photocatalytic degradation of pharmaceuticals in water using MOF-based materials.

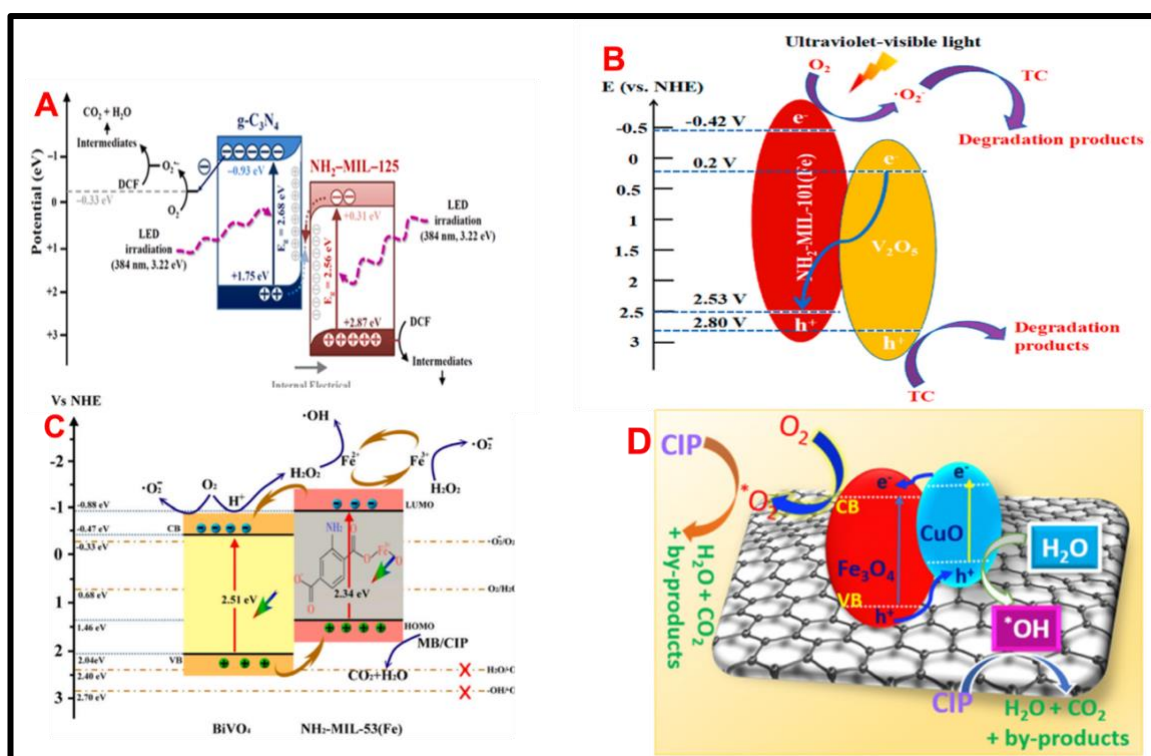


Figure 9: Different schemes for the photodegradation of pharmaceutical pollutants

(A) Proposed S-scheme photocatalytic mechanism for the diclofenac degradation using g-C₃N₄-NH₂-MIL-125 (Muelas-Ramos and Sampaio et al., 2021) (B) Photocatalytic degradation mechanism for Tetracycline over V₂O₅/NH₂-MIL101(Fe) composites (Huang et al., 2021) (C) Proposed mechanism for enhanced degradation of ciprofloxacin (CIP) over BiVO₄/NH₂-MIL-53(Fe) photocatalyst under visible light irradiation (Wang et al., 2021) (D) proposed mechanism for the photocatalytic degradation of ciprofloxacin (CIP) using Fe₃O₄/CuO@C composite and Fe- CuBDC as a template (Le et al., 2021)

1.4.7 Potential Contributions and Limitations of the Study

The significance of the challenges posed by the presence of PCs in wastewater cannot be overstated. Numerous technologies have been utilized to effectively degrade these stubborn pollutants, and photocatalysis (HP) has emerged as a promising environmentally friendly approach for their complete mineralization. A key research focus in HP is the development of advanced photocatalytic materials. As discussed earlier, the utilization of heterojunctions and bandgap engineering represents a promising and emerging strategy for creating highly efficient photocatalytic MOFs. In this study, TiO₂ was combined with NH₂-MIL-125 to form a heterojunction using the solvothermal synthesis technique, for the degradation of Ciprofloxacin, a widely used fluoroquinolone antibiotic. Various TiO₂/MOF composites were fabricated by adjusting the loading of TiO₂. A few research studies have been published using the

same composites for various other applications. For example, Zhang et al. (2018) synthesized $\text{NH}_2\text{-MIL-125@TiO}_2$ core-shell through a post-solvothermal method by further heating the already synthesized MIL MOF in an ethanoic solvent containing thioacetamide at an optimal temperature of 2 h to produce the TiO_2 composite for H_2 production. Song et al. (2019) fabricated $\text{NH}_2\text{-MIL-125(Ti)}$ incorporated TiO_2 nanotube arrays composite anodes for photo-electrocatalytic water splitting. Similar to this work, Ahmedpour et al. (2020) degraded organic dye pollutants in aqueous media using novel calcium-doped $\text{TiO}_2/\text{MIL-125-NH}_2$ which builds upon the in-situ synthesis technique adopted in an earlier work of Fu et al. (2012), although Fu et al. applied the composite for CO_2 reduction. In the present work, the in-situ synthesis of $\text{TiO}_2/\text{NH}_2\text{-MIL-125}$ was followed and a novel material Lanthanum-doped $\text{TiO}_2/\text{NH}_2\text{-MIL-125}$ was synthesized for the photodegradation of ciprofloxacin in water. The research work seeks to contribute to the growing research on pharmaceutical wastewater treatment in the aspect of renewability and sustainability. However, it should be noted that this study's main limitation is that the material's efficiency was primarily demonstrated on a laboratory scale. To validate the potential commercialization of MOF-based materials and their practical implementation on a larger scale, real pharmaceutical wastewater must be utilized.

Table 2: Photocatalytic degradation characteristics for PCs in aqueous media by MOF-based photocatalysts

MOF-based Composite	PC (C₀ [mg L⁻¹])	Catalyst dosage [g L⁻¹]	Lamp emission spectra	Kinetic constant [min⁻¹]	Ref.
V ₂ O ₅ /NH ₂ -MIL-101(Fe)	Tetracycline (-)	0.5	UV+visible	0.018	(Huang et al., 2021)
g-C ₃ N ₄ /ZIF-8	Tetracycline (20)	0.2	Visible	0.035	(Yuan et al., 2021)
g-C ₃ N ₄ /NH ₂ -MIL-125 (Ti)	Diclofenac (10)	0.25	UV	0.029	(Muelas-Ramos and Sampaio et al., 2021)
BiVO ₄ /NH ₂ -MIL-53(Fe)	Ciprofloxacin (10)	0.2	Visible	0.014	(Wang et al., 2021)
BiOI/MIL-121	Tetracycline (20)	1.0	Visible	0.0095	(Dai et al., 2021)
In ₂ S ₃ nanorod/MIL-68-In	Tetracycline hydrochloride (50)	0.3	Visible	0.009	(Fang et al., 2018)
C-TiO ₂ /CoTiO ₃ core/MIL-125/Co	Ciprofloxacin (10)	0.5	Visible	0.046	(Lin et al., 2021)
Co ₃ O ₄ /g-C ₃ N ₄ /MOF-Co nanosheets	Tetracycline (20)	0.2	Visible	0.039	(Jin et al., 2020)

CNT-carbon nanotube, UV-ultraviolet, PC-Pharmaceuticals

Table 3: Photocatalytic degradation characteristics for PCs in aqueous media by MOF-based photocatalysts (Continued)

MOF-based Composite	PC (C_0 [mg L⁻¹])	Catalyst dosage [g L⁻¹]	Lamp emission spectra	Kinetic constant [min⁻¹]	Ref.
Fe ₃ O ₄ /CuO/C Fe-CuBDC	Ciprofloxacin (15)	0.5	Visible	0.035	(Le et al., 2021)
C ₃ N ₄ -TE/TiO ₂ /UiO-66	Tetracycline (20)	0.4	Visible	0.080	(Safaralza deh et al., 2021)
MoS ₂ /ZIF-8	Tetracycline hydrochloride (20)	0.4	Visible	0.0078	(Chen et al., 2019)
CNT/MIL-101 (Fe)	Ciprofloxacin (3.02 ¹)	0.5	Visible	0.051	(Yan et al., 2019)
Fe ₃ O ₄ /SiO ₂ /MIL-53-NH ₂	Ampicillin (100)	0.6	Visible	0.01	(Sohrabnezhad et al., 2020)
CuWO ₄ /Bi ₂ S ₃ /ZIF-67	Metronidazole (20)	0.3	Visible	0.039	(Askari et al., 2020)

CNT-carbon nanotube, UV-ultraviolet, PC-Pharmaceuticals

¹ Concentration in μM

Chapter 2: Materials and Methods

2.1 Materials

The following material was purchased and used with no further purification: 2-Amino terephthalic acid (H_2ATA), titanium tetraisopropoxide (TTIP), TiO_2 anatase, Lanthanum nitrate ($\text{La}(\text{NO}_3)_3 \cdot x\text{H}_2\text{O}$), Ciprofloxacin (CIP), Sodium hydroxide (NaOH), dimethyl formamide (DMF), from Sigma-Aldrich. Methanol from Fisher Scientific.

2.2 Preparation of Photocatalysts

2.2.1 Preparation of TiO_2 Nanowire (NW)

TiO_2NW was prepared hydrothermally from TiO_2 anatase similar to (Zhang et al., 2002). In a typical procedure, 0.5 g of TiO_2 anatase white powder was dissolved in a beaker containing 40 mL of 10 M NaOH. The suspension was stirred for about 30 min then transferred into a 50 mL autoclave. The tightly sealed autoclave was placed in the furnace at 180°C for 24 h. Thereafter, the autoclave was cooled to room temperature. The sample was washed several times with water, and the pH was adjusted by washing with a dilute HCl aqueous solution. The sample was oven-dried at 80°C overnight.

2.2.2 Preparation of $\text{TiO}_2(\text{NW})/\text{NH}_2\text{-MIL-125}$

$\text{NH}_2\text{-MIL-125}$ is a Ti-based MOF synthesized by solvothermal technique using TTIP as the source of Titanium ion and H_2ATA as the linker similar to Ikreedeeh & Tahir (2023). 1.0869 g of H_2ATA was weighed in a dry-cleaned beaker, 18 mL of DMF was added and the mixture was stirred at about 500 rpm on a magnetic stirrer until the solution was clear. 2 mL methanol was added to the solution while stirring, followed by 0.4263 g of TTIP. The mixture was stirred for 30 minutes to achieve a clear yellow solution and then transferred into a 50 mL Teflon autoclave. The autoclave was heated in the furnace for 72 h at 150°C . Thereafter, the suspension formed was cooled and washed twice with DMF, and with methanol about three times to replace the traces of DMF with methanol. The final yellow sample was dried at 60°C for over 12 h. For the synthesis of the $\text{TiO}_2/\text{NH}_2\text{-MIL-125}$, the procedure mentioned above was repeated, except for the addition of 20 mg of TiO_2 NW to the yellow mixture before transferring into the Teflon

autoclave and then subjected to 72 h of heat in the furnace. Eventually, the resulting mixture was washed several times with DMF and methanol and was oven-dried at 60°C overnight. Figure 10 represent the synthesis procedure for the composite.

2.2.3 Preparation of La/TiO₂NW/NH₂-MIL-125

To prepare La/TiO₂/NH₂-MIL-125 photocatalyst with different La concentrations of 5%, 20%, and 30%, different weight percentages of the Lanthanum in Lanthanum nitrate (La(NO₃)₃.xH₂O) were used. For a typical La concentration, the weight fraction is measured and dissolved in methanol on stirring, the corresponding mass of synthesized TiO₂/NH₂-MIL-125 is added and stirred for about 2 h. The methanolic suspension is then dried at 60°C overnight.

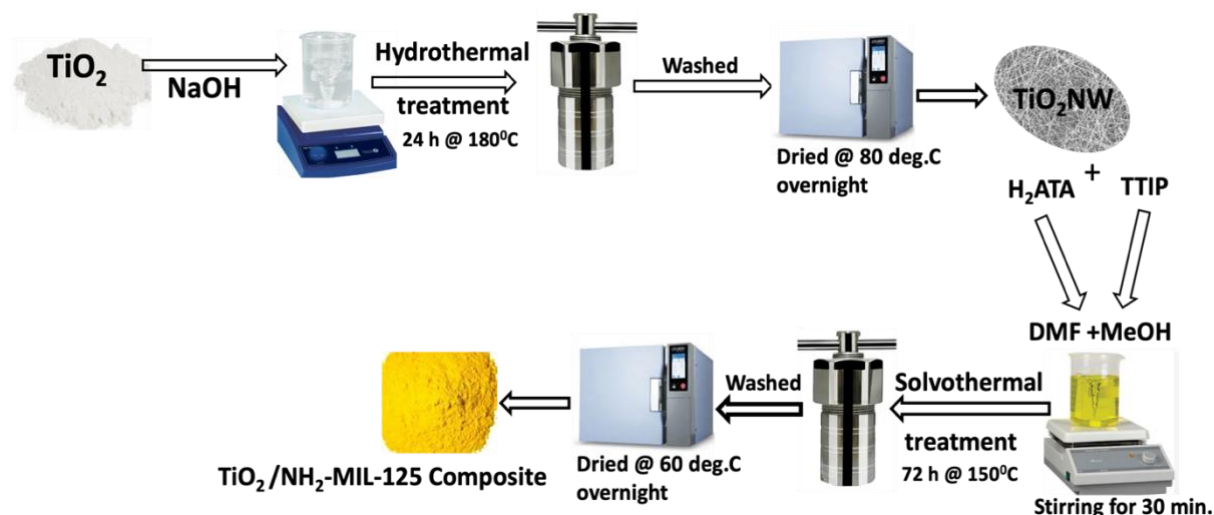


Figure 10: A systemic demonstration for the synthesis of TiO₂/NH₂-MIL-125 composite

2.3 Characterization of Synthesized Photocatalysts

The synthesized materials characterization was carried out by various laboratory-scaled equipment to determine both structural and chemical features. X-ray diffraction (XRD) (Shimadzu-6100 X-ray diffractometer using Cu-K α radiation with a wavelength of 1.542 Å) was used to determine the crystalline structure of the synthesized photocatalysts. Scanning electron microscopy (SEM) was performed using a Hitachi S-4800 scanning electron microscope (Hitachi, Tokyo, Japan) at an acceleration voltage of 15 kV. The chemical features of the synthesized materials were determined by Fourier

Transform Infrared Spectroscopy (FTIR) (Thermo Nicolet, NEXUS 470 FT-IR Spectrophotometer). Using a UV-Vis spectrophotometer (Shimadzu, UV-2550, Japan), the UV-Vis spectra of the specimens were measured. A TriStar II PLUS (Micromeritics) was used to assess the porous texture by N₂ adsorption-desorption at – 196 °C. The samples were previously outgassed under vacuum at 150 °C. The Brunauer-Emmet-Teller method by Walton & Snurr (2007) was used to calculate the specific surface area (S_{BET}). Total pore volume (V_T) was determined by the amount of N₂ adsorbed at 0.99 relative pressure (P/P_0). Micropore volume (V_{MP}) was obtained from the t-plot method (Howarth et al., 2017). The pore size distribution was determined by the Barrett-Joyner-Halenda Model (BJH) model. A Spectrofluorescence instrument (Shimadzu (RF-6000 Series)), set at an excitation wavelength of 310 nm was employed to measure the fluorescence emission spectra.

2.4 Photocatalytic Reactivity Test

Batch experiments were performed in a 150 mL reactor containing 100 mL of CIP solution (10 mg/L) and 20 mg photocatalyst at room temperature. A 200 W Xenon arc lamp (Generic HID MB-9005 with a color temperature of 6000 K) was used as the light irradiation source. In a typical experiment, 20 mg of photocatalyst La/TiO₂/NH₂-MIL-125 was added to 100 mL of CIP solutions with an initial concentration of 10 mg/L. The reactor containing the CIP solution and the catalyst was covered with aluminum foil while being stirred continuously until adsorption equilibrium was established in the dark after 60 min. Then, the light was switched on and the reaction was followed for 90 min. Aliquots were taken at 10 min time intervals in the first 30 min and filtered with PTFE syringe filters (0.22 µm) to separate the solid photocatalyst. The reaction temperature was carried out at room temperature. The CIP concentration was analyzed by a spectrophotometer (Bioevopeak, Double Beam UV-Vis Spectrophotometer SP-IUV7). The characteristic wavelength for CIP was determined at 277 nm. The percentage CIP photodegraded was calculated based on the efficiency of the photocatalyst using Equation (1):

$$\text{Pollutant removal (\%)} = \frac{C_0 - C_t}{C_0} \times 100 \quad (1)$$

Where C_0 is the initial pollutant concentration in water and C_t is the concentration at time t (min). To estimate the reaction rate constant, a pseudo-first order rate of reaction was employed to model the pollutant removal from water as shown in eq. 2a.

$$r_{PC} = -\frac{dC}{dt} = kC \quad (2a)$$

Where r_{PC} is rate of reaction of the PC and k is the observed pseudo first order reaction rate constant (min^{-1}). From eq. 2a, the eq. 2b can be obtained as shown below.

$$-\ln\left(\frac{C_t}{C_0}\right) = kt \quad (2b)$$

Chapter 3: Results and Discussions

3.1 Characterization of the Photocatalysts

3.1.1 X-ray Diffraction Analysis

Figure 11 provides insights into the structural characteristics of the various catalysts under examination (bare $\text{NH}_2\text{-MIL-125}$ (labeled NHM), TiO_2 nanowire (labeled TiO_2NW), $\text{TiO}_2/\text{NH}_2\text{-MIL-125}$ composite (labeled TNHM), and Lanthanum doped composite (labeled LaTNHM30)). The X-ray diffraction (XRD) patterns reveal distinct peaks that are indicative of specific crystalline phases. The XRD pattern of the as-synthesized TiO_2NW exhibits characteristic peaks at 2θ values of 25.22° , 39.04° , and 48.72° , corresponding to the (101), (004), and (200) planes of the anatase phase of TiO_2 , respectively. This aligns well with the JCPDS 21-1272 database (Chang et al., 2017), confirming the successful synthesis of TiO_2 NW. Furthermore, the synthesized $\text{NH}_2\text{-MIL-125}$ and its composites display peaks at 2θ values of 6.8° , 9.5° , and 11.6° , corresponding to the (011), (020), and (121) planes of $\text{NH}_2\text{-MIL-125}$ (Muelas-Ramos and Belver et al., 2021). These peaks affirm the retention of the crystalline phase of $\text{NH}_2\text{-MIL-125}$ within the composites, indicating the structural integrity of the MOF.

Importantly, the relatively weak intensity of TiO_2 peaks in the $\text{TiO}_2/\text{NH}_2\text{-MIL-125}$ composite is attributed to the limited amount of assembled TiO_2 on $\text{NH}_2\text{-MIL-125}$, as visually confirmed by SEM images. Conversely, the Lanthanum-doped composites exhibit more intense peaks in the (121) plane of $\text{NH}_2\text{-MIL-125}$ and the (100) plane of TiO_2 . This observation suggests a potential interaction between Lanthanum species and the catalyst components. Notably, this phenomenon aligns with a similar finding reported by Lu et al (2018) during the La doping of HZSM-5 zeolite catalyst, where broad XRD signals at $2\theta = 28.1^\circ$, 39.4° , and 49.0° indicated the presence of Lanthanum species.

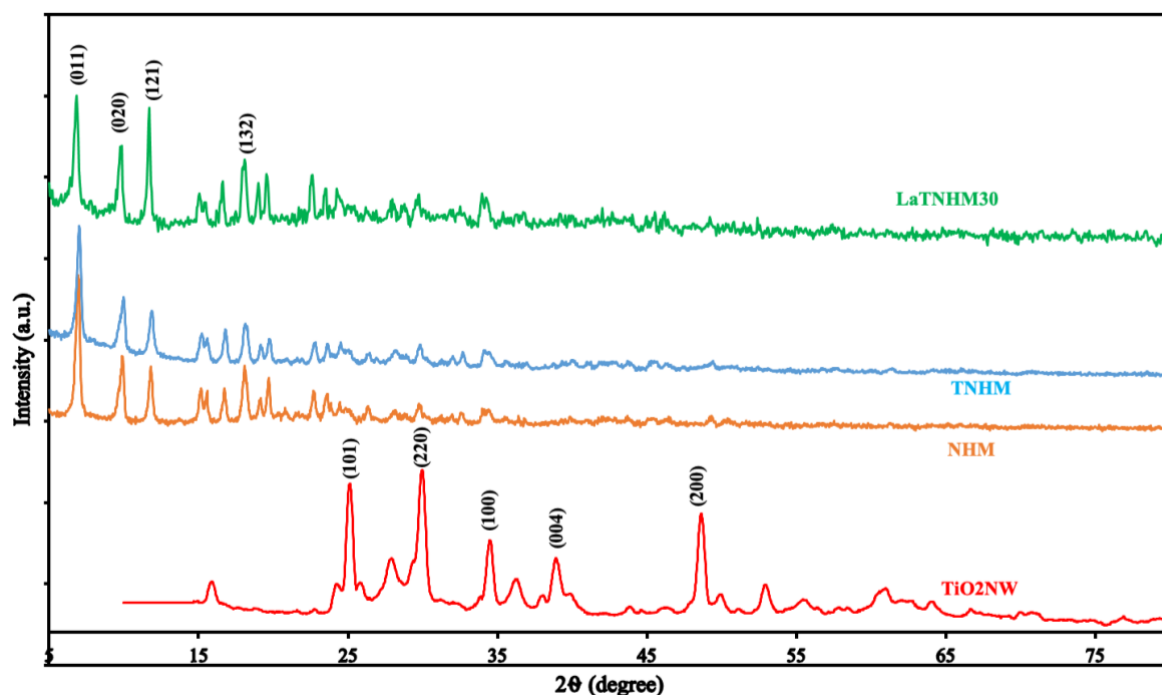


Figure 11: X-ray diffraction patterns of synthesized photocatalysts

3.1.2 Scanning Electron Microscopy (SEM) Analysis

Complementing the XRD analysis, SEM images (Figure 12) offer a visual confirmation of the structural morphology of the catalysts. They clearly depict the presence of nanowire-like TiO_2 structures assembled on the MOF surface. These nanowires are distinctly visible on the surface of the rectangular disk-like MOF particles. The SEM analysis provides valuable insights into the morphology and distribution of TiO_2 within the $\text{TiO}_2/\text{NH}_2\text{-MIL-125}$ composite. While SEM is informative for visualizing morphology, it may not always capture the presence of certain elements, such as Lanthanum. In this case an Energy-Dispersive X-ray (EDX) analysis is required to provide a more accurate assessment of the Lanthanum content in the LaTNHM30 composite.

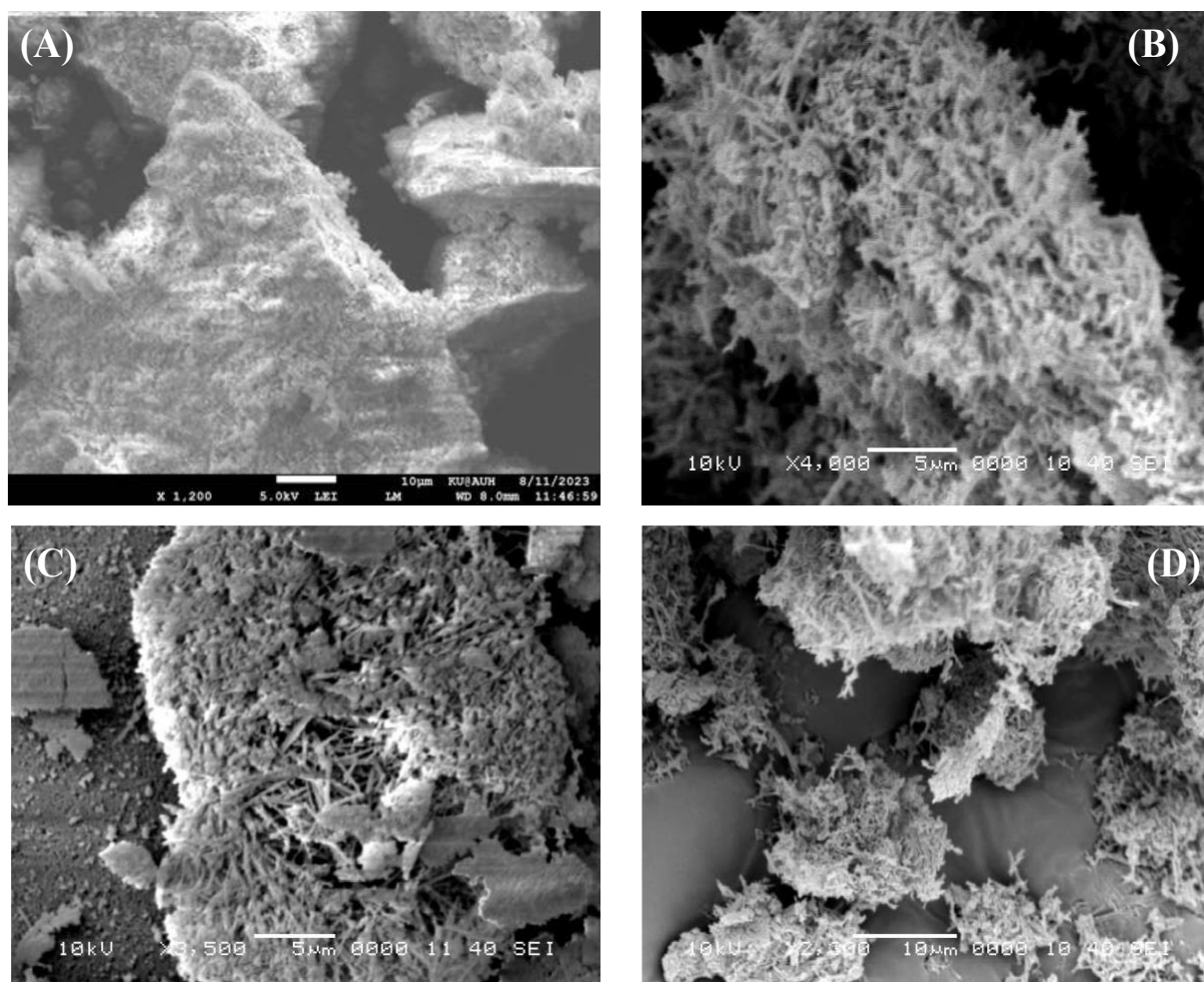


Figure 12: SEM images

(A) $\text{NH}_2\text{-MIL-125}$ (B) agglomeration of TiO_2NW (C) $\text{TiO}_2\text{NW}/\text{NH}_2\text{-MIL-125}$ (D) Agglomeration of TiO_2NW within the $\text{NH}_2\text{-MIL-125}$ cavity

3.1.3 Fourier Transform Infrared (FTIR) Analysis

The FTIR analysis delves into the surface chemistry and functional groups present in the catalysts (Figure 13). A comparative examination of the FTIR spectra across various photocatalysts enables us to identify and discuss specific vibrations and chemical bonds. The FTIR spectrum of TiO_2NW aligns with previous studies (Chougala et al., 2017) exhibiting distinct peaks such as the Ti-O bending mode at 422 cm^{-1} , the deformative vibration of the Ti-OH stretching mode at around 1630 cm^{-1} , and the stretching vibrations of -OH groups at 3149 cm^{-1} . These peaks are consistent with the known characteristics of TiO_2 . In the case of $\text{TiO}_2/\text{NH}_2\text{-MIL-125}$, the FTIR spectrum reveals peaks at 1255 , 1380 , 1542 , and 1655 cm^{-1} . These peaks correspond to vibrations of carboxylate groups, O-Ti-O vibrations, and the stretching vibrations of C-N bonds

from aromatic amine groups. These findings align with prior research by Zhao et al. (2019) and further affirm the presence of specific functional groups within the $\text{TiO}_2/\text{NH}_2\text{-MIL-125}$ composite.

Interestingly, the FTIR spectrum of the La-doped composite exhibits similar peaks to those observed in $\text{TiO}_2/\text{NH}_2\text{-MIL-125}$. This suggests that the addition of Lanthanum does not induce significant alterations in the $\text{TiO}_2/\text{NH}_2\text{-MIL-125}$ structure. Notably, weak bands at 2426 cm^{-1} are observed in the LaTNHM30 spectrum, which may be associated with La-O-Ti or La oxide species (Quan et al., 2007; Xu et al., 2002). These findings warrant further confirmation through X-ray Photoelectron Spectroscopy (XPS) characterization.

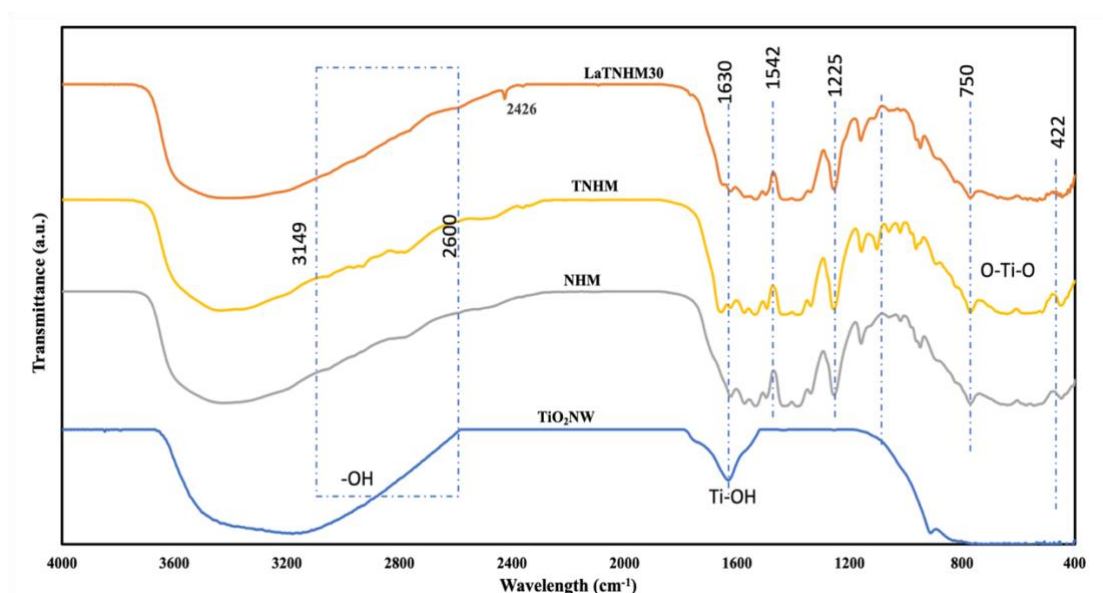


Figure 13: FTIR analysis of synthesized photocatalysts

3.1.4 Textural Characterization and N_2 Physisorption

In order to comprehensively assess the textural properties of both the synthesized MOF and the MOF composite, N_2 physisorption characterization was conducted. The N_2 adsorption-desorption isotherms, as depicted in Figure 14, reveal the presence of microporous structures, and highlight specific microporosity properties, along with a high surface area. It is noteworthy, however, that the Surface Area (S_{BET}) calculation was not performed for the synthesized MOF. This omission was due to equipment

limitations, particularly concerning the handling of highly microporous solids, as is the case with $\text{NH}_2\text{-MIL-125}$ nanoparticles. The isotherms for the $\text{TiO}_2\text{-MOF}$ composite exhibit a similar pattern to those of the pure MOF. However, there is a discernible decrease in pore volume and Langmuir surface area (Table 3). This reduction can likely be attributed to the agglomeration of TiO_2NW on the surface and within the pores of the MOF, a phenomenon visually confirmed by the SEM images. Additionally, the Barrett-Joyner-Halenda (BJH) pore size distribution model shows a small displacement of the composite sample towards narrower microporosity, which might be due to the residual presence of excess linker or solvent that may not have been completely removed during the washing process (Muelas-Ramos and Belver et al., 2021).

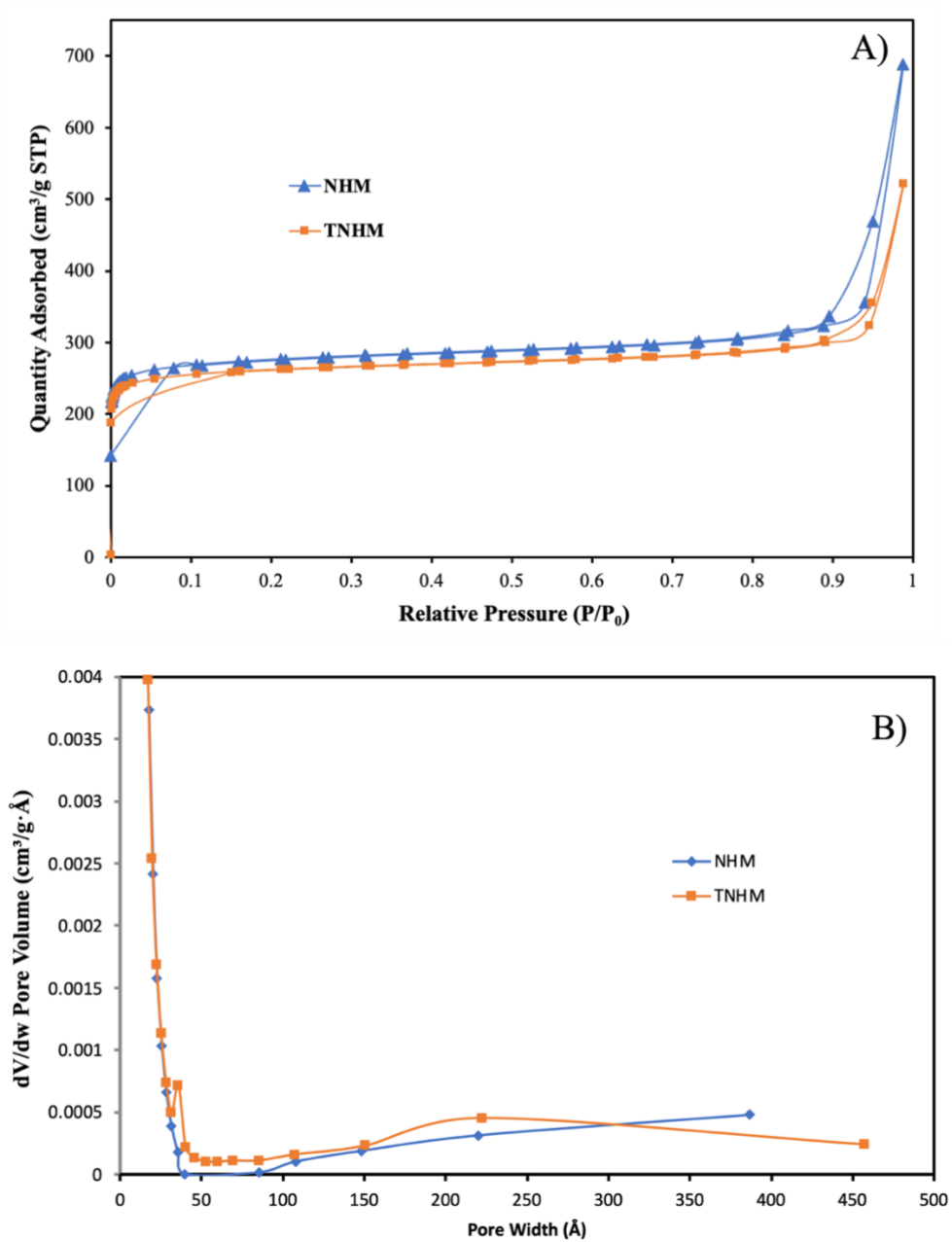


Figure 14: S_{BET} analysis for NH_2 -MIL-125 and TiO_2/NH_2 -MIL-125 composite

A) N_2 adsorption-desorption isotherms and B) Pore size distributions from Barrett-Joyner-Halenda (BJH) model

Table 4: Porous texture, average pore diameter, and volume

Photocatalyst	Langmuir Surface Area (m ² /g)	TPV (cm ³ /g)	APD (nm)
NHM	1697	0.6957	21.75
TNHM	1507	0.4493	15.84

TPV - Total Pore Volume, APD - Average Pore Diameter

3.1.5 UV-Vis Spectroscopy and Band Gap Calculation

The optical properties of the prepared samples were analyzed via UV–vis Diffuse Reflectance Spectroscopy (DRS) (Figure 15). The spectra for TiO₂NW and those of the MOF and its composites are presented in Figure 15A and 15C respectively. TiO₂NW exhibits a single absorption band centered at 270 nm. In contrast, NHM, TNHm, and LaTNHM photocatalysts display nearly identical absorption intensities centered at approximately 280 and 370 nm. These absorption bands can be attributed to the presence of Ti-oxo-clusters and linker components, as previously reported (Muelas-Ramos and Belder et al., 2021). Notably, both the MOF and MOF composite samples exhibit enhanced absorption in the visible range. This enhancement can be attributed to the reduced HOMO-LUMO gaps, a result of amine modification in MIL125. However, the absorption pattern displayed by the La-doped composite suggests the formation of Schottky junctions, likely facilitated by charge transfer interactions between the TiO₂ and Lanthanum. Interestingly, no plasmonic band associated with Lanthanum was observed. This absence may be due to the low Lanthanum content and its highly hygroscopic nature.

The determination of band gap energies (E_g) via the Tauc plot method (Figure 15B and 15D) is pivotal in understanding the electronic properties of the photocatalysts. As anticipated, TiO₂NW exhibits a relatively wide band gap of 3.3 eV. Conversely, the

MOF-derived photocatalysts yield band gap values ranging from 2.45 to 2.52 eV. For the pure MOF, the band gap was estimated to be 2.5 eV. Interestingly, the presence of TiO_2 in the MOF composites results in a slight increase in the band gap to 2.52 eV. However, upon doping with Lanthanum, the band gap decreases to 2.45 eV. This minor difference in band gap values indicates that the incorporation of Lanthanum metal into the MOF sample does not disrupt the band gap properties of the MOF.

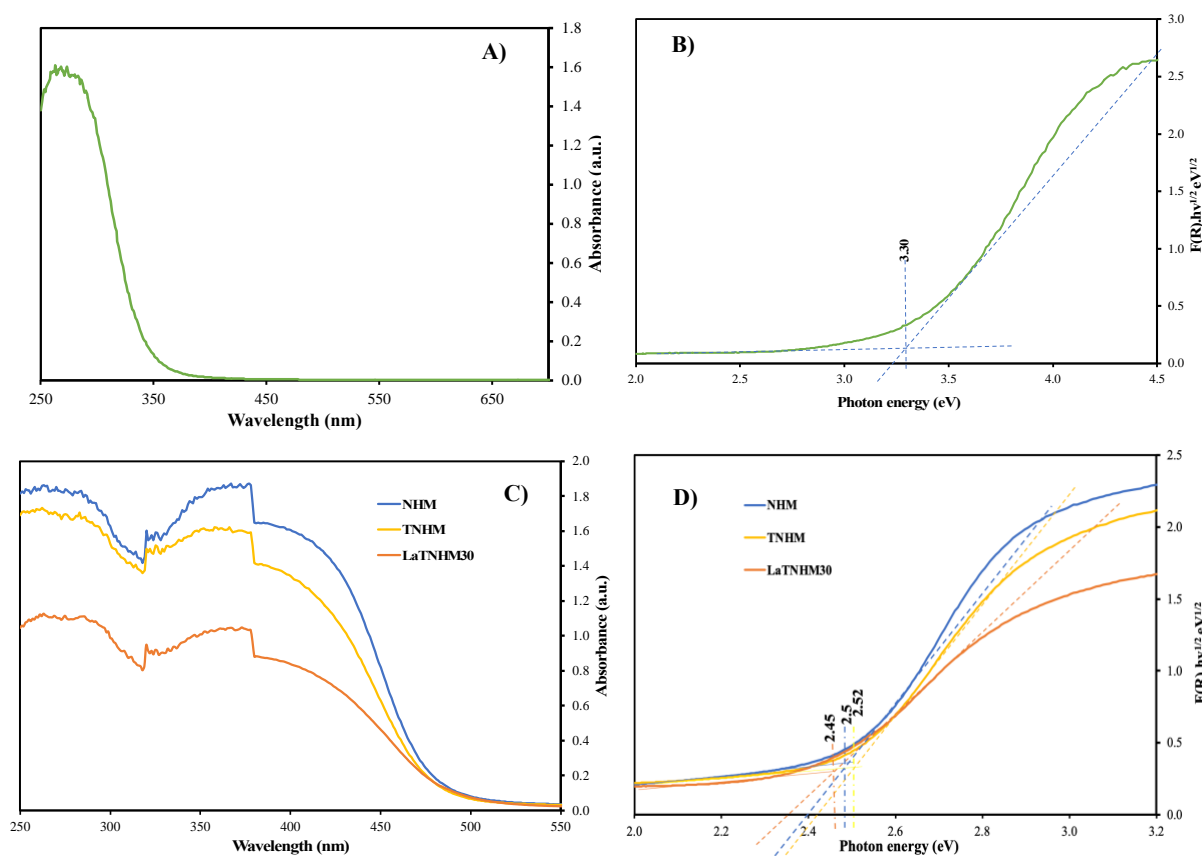


Figure 15: UV-VIS DRS spectra and Tauc plots

A) UV-Vis DRS Spectra of TiO_2NW and B) Tauc plots of TiO_2NW C) UV-Vis Spectra of NHM, TNHMs, and LaTNHM D) Tauc plots of NHM, TNHMs, and LaTNHM

3.1.6 Fluorescence Emission Spectra

To gain insights into the electron transfer behavior of the photocatalysts, fluorescence emission spectra were analyzed using a spectrofluorometer. The excitation wavelength was set at 310 nm for all photocatalysts, and the emission wavelength was scanned from 310 to 800 nm. As illustrated in Figure 16, a prominent fluorescence peak

in the range of 565 to 600 nm is observed for TiO₂NW. This peak shifts slightly to the right, ranging from 600 to 640 nm, for NHM, TNH, and LaTNH. This shift indicates a longer emission wavelength and, consequently, higher energy dissipation in TiO₂NW due to rapid recombination. Notably, NHM exhibits intense peaks within the 410 to 490 nm range, suggesting recombination rates of electron-hole pairs. Comparatively, the fluorescence intensity of TNH decreases, while that of LaTNH is negligible. This observation implies that the introduction of TiO₂NW enhances the separation efficiency of NHM, and this is further improved by metal doping. The minimal peak intensity observed in the LaTNH30 emission spectrum suggests that the rate of electron-hole recombination is at its lowest. This can be attributed to the reduced presence of trapping sites for electrons involved in light emission (Ahmadpour et al., 2020).

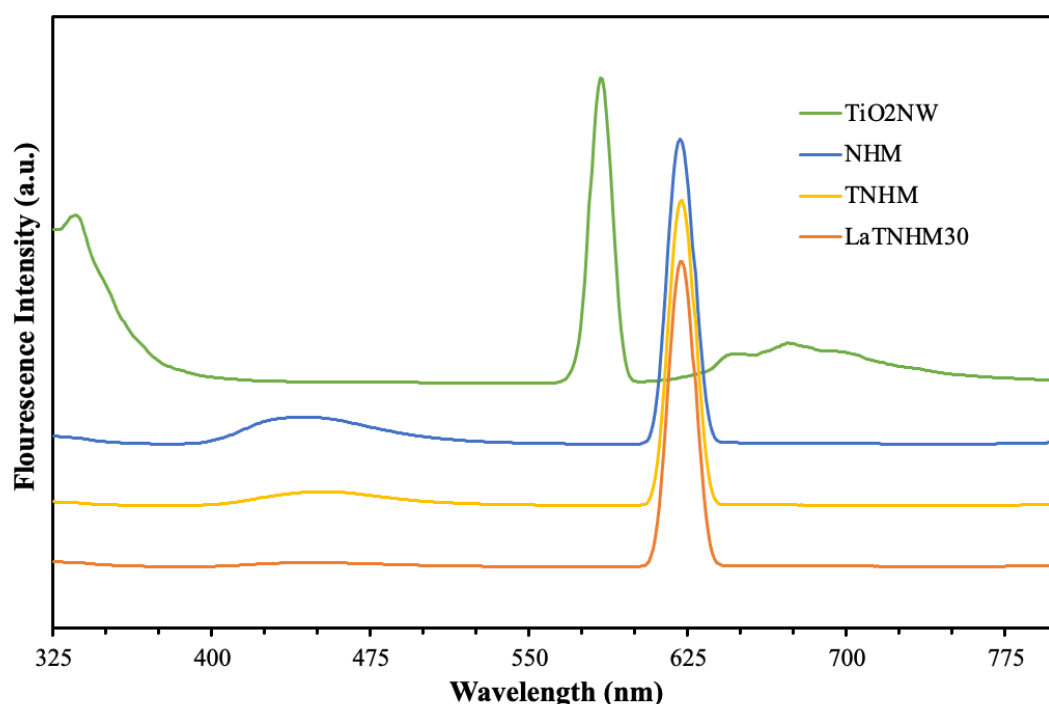


Figure 16: Fluorescence emission spectrum of photocatalysts in spectrofluorometer

Experimental parameters: $\lambda_{\text{ex}} = 310 \text{ nm}$, $\Delta\lambda_{\text{ex}} = 5 \text{ nm}$, $\Delta\lambda_{\text{em}} = 5 \text{ nm}$, solvent: ethanol

3.2 Photocatalytic Efficiency Study

In order to understand the stability of CIP in the presence of solar light, a preliminary photodegradation test was conducted without the use of a catalyst. Unfortunately, the researchers observed negligible degradation of CIP under solar light, as shown in Figure 16B.

Prior to proceeding with the reaction test, the research team evaluated the CIP adsorption-desorption performance of the photocatalysts. Specifically, 30 mg of each photocatalyst was dispersed in 100 mL of 20 ppm CIP solution and allowed it to remain in the dark for 90 minutes (Figure 17A). The adsorption-desorption equilibrium was reached in about an hour for NHM and TNH, while TiO₂NW exhibited quicker adsorption with a lower value. Notably, pure MOF (NHM) displayed a high adsorption rate of 60% after 60 minutes, whereas the MOF composite (TNH) showed a lower adsorption rate of 40%. These adsorption values were taken into consideration to adjust the initial pollutant concentration to 10 ppm and a photocatalyst loading of 0.2 g/L. A pH of approximately 3.7 was maintained due to the acidic nature of the CIP solution. The investigation then proceeded to assess the photocatalytic degradation of CIP using TiO₂NW, pure MOF (NHM), MOF composite (TNH). As shown in Figure 17B, the photocatalytic performance of the TNH photocatalyst was the highest at 0.0111 min⁻¹, compared to bare MOF and TiO₂NW. This result aligns with previous studies (Ahmadpour et al., 2020; Huang et al., 2019; Song et al., 2019; Zhang et al., 2018; Zhang et al., 2016).

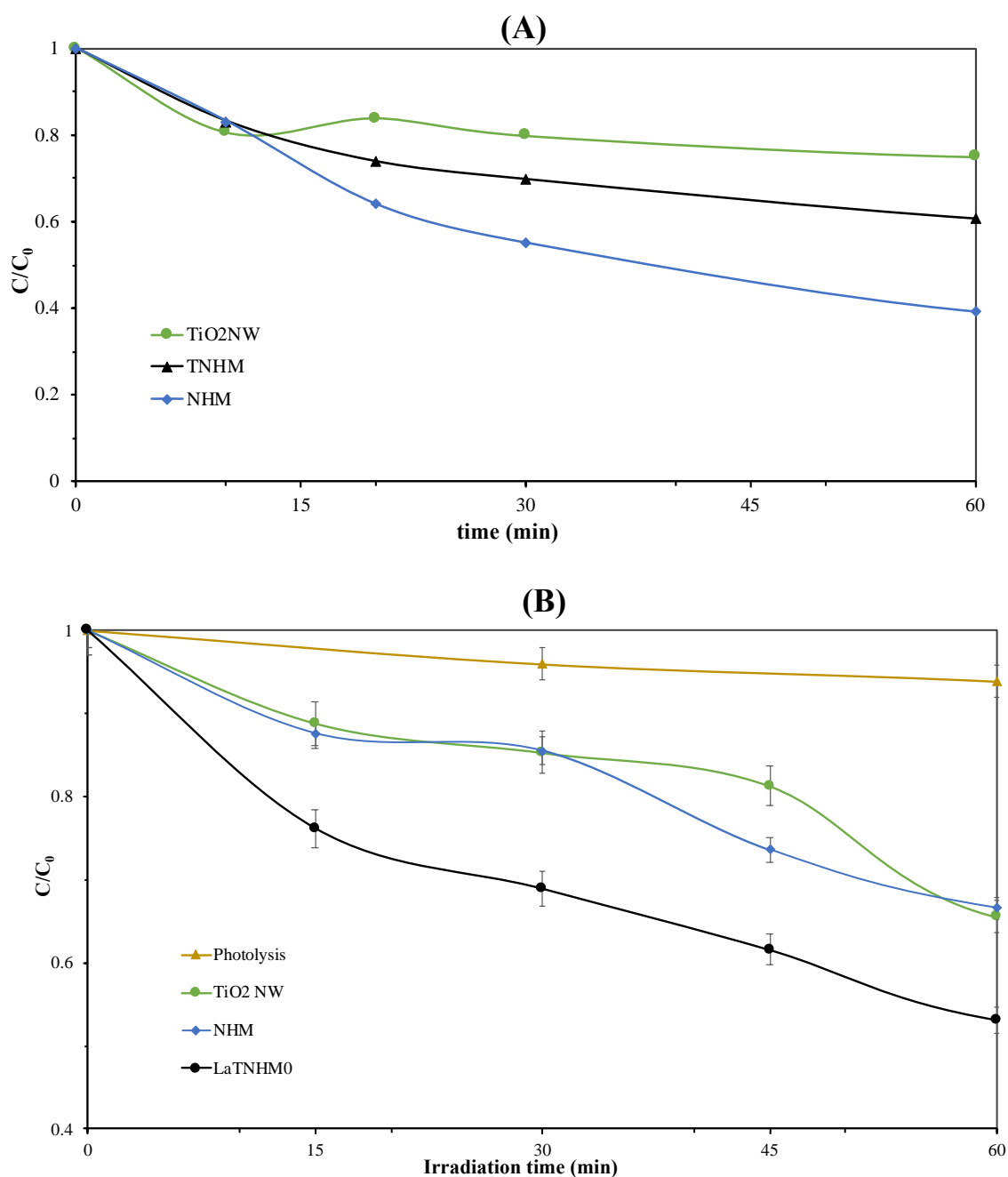


Figure 17: Removal of the CIP pollutant in water

A) dark stage B) under solar irradiation with the photocatalysts tested ($[CIP]_0 = 10 \text{ mg L}^{-1}$; Photocatalyst load = 200 mg L^{-1} ; 200 W Xenon light)

3.3 Optimization of Selected Parameters

In this section, the various parameters considered for the photodegradation of CIP by the synthesized nanocomposites are presented.

3.3.1 Effect of Illumination Configuration

Before conducting the photocatalytic reaction tests, we carefully considered the experimental setup. Photoreactors are critical in the photocatalytic process and serve as essential engineering components. Factors such as improving light absorption, minimizing photon losses, and enhancing product separation and charge carrier recombination are crucial for designing more efficient photoreactors (Nguyen & Wu, 2018). Therefore, creating an appropriate reactor is essential for optimizing selectivity under various conditions. Initially, an internally illuminated slurry reactor was considered. This choice is known for its advantages in photocatalysis, such as improved light penetration and distribution. However, it's important to control light intensity and heat, depending on the photocatalytic nature of the catalyst. In this work, the light source was a 200 W xenon light with an unknown light intensity. Notably, xenon lamps emit a predominantly continuous and consistent spectrum across the entire visible range, with a color temperature of around 6000 K, resembling sunlight and having no prominent emission lines. Nevertheless, only a quarter of the total light output is in the visible range, with the majority being in the less practical infrared spectrum, and less than 5 percent falling within the ultraviolet spectrum. It was observed that the chosen light source had the capability to raise the reaction temperature to as high as 60°C after 60 minutes of reaction (refer to Figure 18 and Figure 19). The effect of the temperature increase on the catalyst's performance became evident after 60 minutes of irradiation. Due to the inability to control both the light intensity and the rate of heating, the reaction setup was modified to utilize side illumination (photo not shown) in the absence of lamp cooling system. This adjustment resulted in an additional 30 minutes of stability in the degradation process before thermal heating began to affect the reaction performance. As shown in Figure 19, the efficiency of the MOF photocatalyst improved significantly upon changing from internally illuminated to externally illuminated. However, it cannot be concluded that the experimental setup is the optimal setup for the reaction as it can be observed that the concentration started to increase again at 90 minutes, implying the effect of thermal heating on the catalyst performance was not eliminated.



Figure 18: Internally illuminated photoreactor heating up after 60 min of reaction.

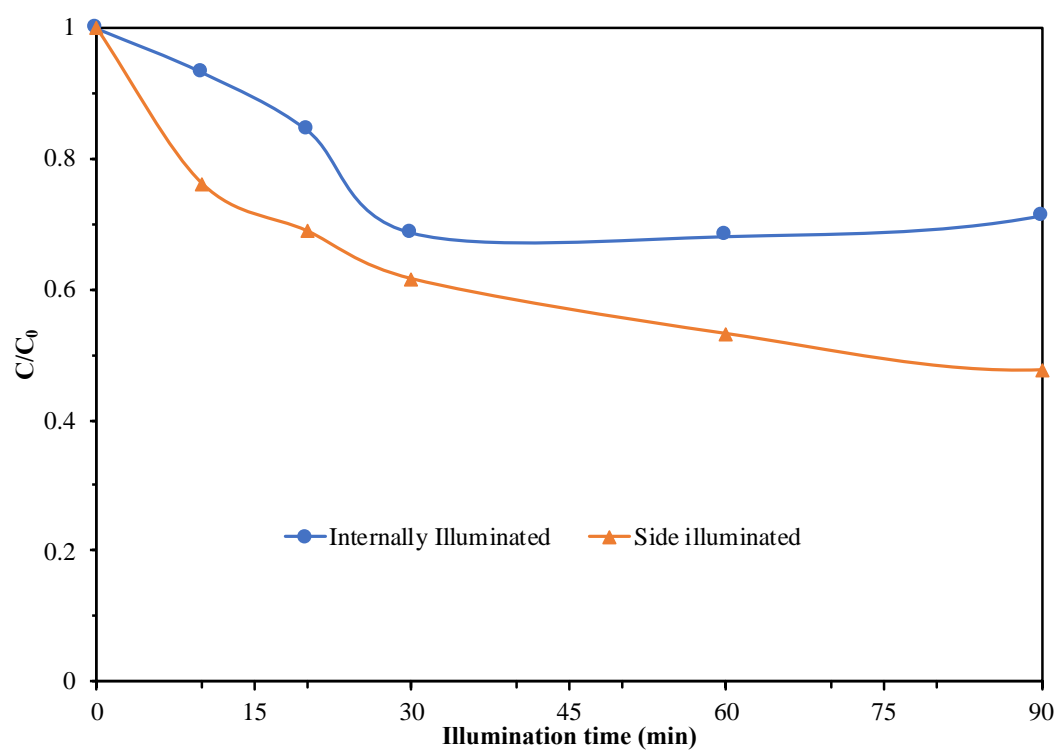


Figure 19: Effect of the illumination configuration on CIP photodegradation using $\text{NH}_2\text{-MIL-125}$

3.3.2 Effect of Initial Concentration of CIP Solution

It was observed that the CIP solution with a concentration of 20 ppm exhibited a slower degradation rate compared to the 10 ppm solution. When a catalytic loading of 0.2 g/L (pure MOF) was used, adsorption equilibrium was achieved much faster, in just 30 minutes, with approximately 20% of CIP being photodegraded. In contrast, when a 10 ppm solution was tested with the same catalytic loading, the degradation efficiency doubled (Figure 20). It is important to note that lower initial concentration values were not investigated, so it cannot be concluded that 10 ppm is the optimal initial concentration. However, the expected concentration of CIP pollutants found in the literature falls within this range.

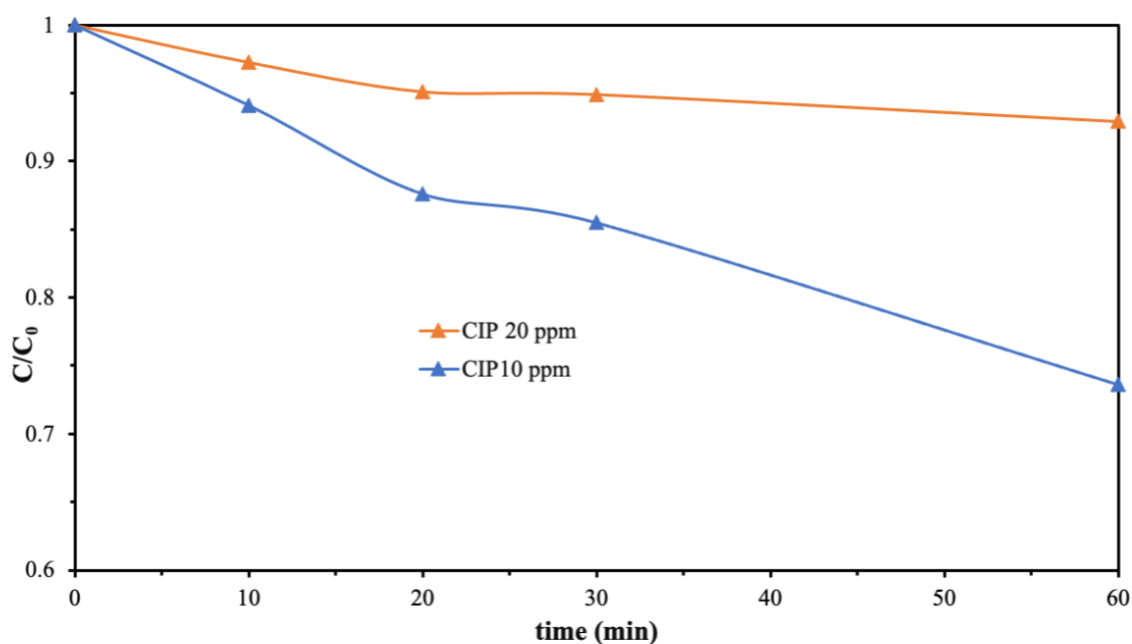


Figure 20: Effect of initial CIP concentration using NH₂-MIL-125

3.3.3 Effect of Metal Doping

In addition to investigating the efficiency of the TiO₂/MOF photocatalyst on the removal of CIP from water, the effect of doping the synthesized composite was explored. Selected compositions of La-doped TNHMs (LaTNHM) of 5%, 20 %, and 30% were synthesized as previously stated in chapter 2. Following the same experimental

procedure for testing the application of TiO₂NW, NHM, and TNHMs, LaTNHM performance was studied.

As shown in Figure 21, the performance increases with increasing La composition with LaTNHM30 exhibiting the highest degradation rate at 42.7% ($k = 0.0067 \text{ min}^{-1}$) amongst other La-doped composites. However, when compared to pure MOF and TNHMs composite, 30% La doping resulted in lower photodegradation than TNHMs but higher than pure NHM.

The performance of the La-doped photocatalysts was inconsistent with previous research on metal doping of TiO₂/MOF composites (Ahmadpour et al., 2020). Even though all characterization results for LaTNHM were consistent with TNHMs and NHM. Consequently, a reasonable inference for this result could be attributed to limitations in the experimental setup. Furthermore, it is important to acknowledge the scarcity of existing literature on Lanthanum as a doping metal. In the few instances where Lanthanum metal has been employed for similar purposes, the decomposition of Lanthanum compounds played a significant role in the doping effect. (Lu et al., 2018; Quan et al., 2007). In the case of this work, anhydrous lanthanum nitrate is the parent compound, implying its decomposition into lanthanum oxide, nitric oxide, or other lanthanum oxide species. Muelas-Ramos and Beller et al. (2021) reported the detrimental effect of common inorganic ions such as nitrate ions on the photocatalytic degradation of acetaminophen. The nitrate ions can react with hydroxyl radicals, resulting in a negative synergistic effect.

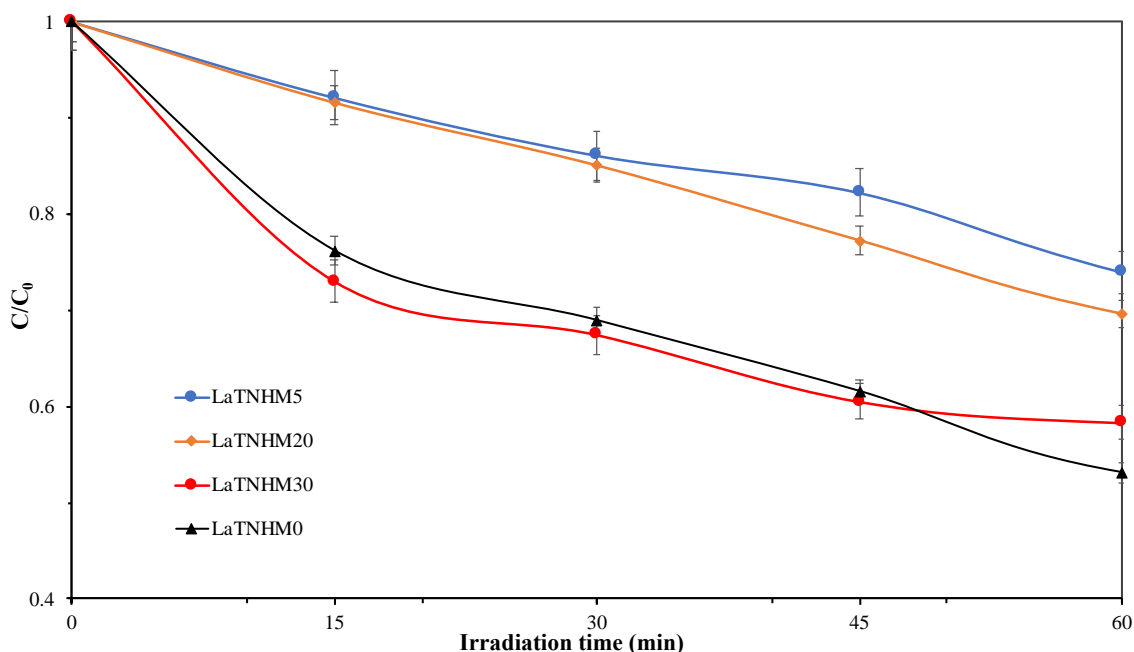


Figure 21: Effect of doping TNHMs with Lanthanum metal at 5%, 20%, 30% La composition.

3.4 Reaction Kinetics

The photodegradation of CIP follows a pseudo-first-order rate equation as represented by Equation 2 (see Appendix for data plots). The rate constants for each prepared photocatalyst are presented in Table 4, along with their corresponding R-squared values. As anticipated, the Lanthanum-doped photocatalyst exhibited lower rate constants when compared to the pure MOF and TiO₂/MOF composite. In contrast, the TNHMs composites displayed the highest rate constant, surpassing that of the bare MOF, NH₂-MIL-125, by a factor of 1.7. This enhancement can be attributed to improved light absorption in the visible spectrum, as demonstrated in the UV-VIS spectra, and reduced charge recombination, as evidenced by the fluorescence spectra.

It is noteworthy that the *k*-value for NH₂-MIL-125 obtained in this study competes that reported by Muelas-Ramos and Belver et al. (2021) for the photodegradation of acetaminophen. Acetaminophen, belonging to a class of pharmaceutical analgesics, is typically less persistent in wastewater treatment than antibiotics. This suggests that NH₂-MIL-125 holds significant potential for the photodegradation of antibiotics. Clearly, the photocatalytic properties of MOF can be

enhanced through the formation of a heterojunction with an inorganic photocatalyst like TiO_2 . To provide context within the specific area of CIP photodegradation, the k-values obtained in this work are compared with previous studies, as summarized in Table 5. As indicated in the table, the photocatalysts developed in this study demonstrate promising and competitive performance relative to prior research.

Table 5: Rate constant values and their R-squared for the tested photocatalysts

Photocatalysts	k (min⁻¹)	R-Squared
TNHM	0.0111	0.9836
NHM	0.0066	0.999
LaTNHM30	0.0067	0.991
LaTNHM20	0.0059	0.9985
LaTNHM5	0.0048	0.9954

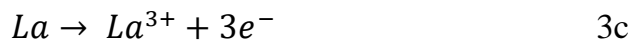
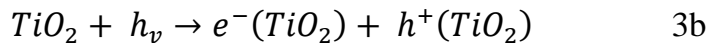
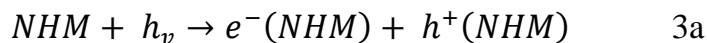
Table 6: Comparative data for the removal of CIP in water by various photocatalysts

Photocatalyst	Irradiation (min)	CIP concentration (mg/L)	Dosage (g/L)	k (min ⁻¹)	Ref.
BiOCl/Bi ₂ WO ₆	300	10	1	0.0035	(Ma et al., 2016)
BiOI/MIL88B(Fe)	270	10	0.3	0.0060	(Islam et al., 2017)
g-C ₃ N ₄ /rGO/WO ₃	180	20	0.2	0.0105	(Lu et al., 2019)
Pt/N-BiOCl	150	10	0.2	0.0114	(Maimaitizi et al., 2020)
Bi ₄ O ₅ Br ₂	120	10	0.5	0.0116	(Di et al., 2015)
CNT/PbBiO ₂ Br	150	10	0.3	0.0141	(Wang et al., 2019)
BiOBr/Bi ₂ MoO ₆	120	10	0.2	0.0158	(Wang et al., 2017)
CQDs/PbBiO ₂ Cl	75	10	0.3	0.0208	(Sheng et al., 2019)
CeO ₂ -Ag/AgBr	120	10	1	0.0223	(Wen et al., 2018)
CuS/BiVO ₄	90	10	1	0.0224	(Lai et al., 2019)
BU-5	120	10	0.75	0.0270	(Zhao et al., 2021)
TiO ₂ /NH ₂ -MIL-125	60	10	0.2	0.0111	This work
La(30)/TiO ₂ /NH ₂ -MIL-125	60	10	0.2	0.0067	This work

3.5 Mechanism of Photodegradation

Although a broader investigation of the reaction intermediates is required to ascertain the reaction pathway, a proposed mechanism is presented based on the preliminary results collected from this work. Assumptions are made according to expected outputs compared to similar published articles such as (Ahmadpour et al., 2020; Muelas-Ramos and Belver et al., 2021). As for the TiO₂NW/NH₂-MIL-125 heterojunction constructed in this work, if a conventional type II heterojunction was formed under white light illumination, both NH₂-MIL-125 and TiO₂NW generate

photoexcited carriers as represented in Equations 3a and 3b. Lanthanum, as a metal in its ionic stage loses electrons as in Equation 3c.



Since the conduction band energy of NH₂-MIL-125 is more negative, the photo-generated electrons undergo migration from the LUMO of NH₂-MIL-125 to the CB of TiO₂NW, whereas transport holes occurred from the VB of TiO₂NW to HOMO of NH₂-MIL-125. This kind of charge transfer configuration was bound to the weak oxidation ability of the holes and decreased reduction ability of the electrons. More importantly, the CB accumulated electrons of TiO₂NW and the holes occupying HOMO of NH₂-MIL-125 cannot reduce O₂ to form •O₂⁻ and oxidize H₂O to produce •OH because $E^0(O_2/\dot{O}_2^-)$ is more negative than E_{CB} of the TiO₂/NH₂-MIL-125 composite and $E^0(H_2O/\bullet OH)$ is more positive than the E_{VB} of the TiO₂/NH₂-MIL-125. Based on the explanation, a Z-scheme charge transfer process is an appropriate approach to understanding the improved photocatalytic efficiency of the TiO₂/NH₂-MIL-125 heterojunction.

As shown in Figure 22, upon absorption of light energy, the photo-generated electrons in the CB of TiO₂NW were inclined to be transferred into the HOMO of NH₂-MIL-125 due to strong electrostatic attraction between the electrons in the CB of TiO₂NW and holes in HOMO of NH₂-MIL-125. In that way, the space separation of photo-generated electron-hole pairs can be remarkably improved within TiO₂NW and NH₂-MIL-125. Therefore, the electrons retained in the LUMO of NH₂-MIL-125 were more susceptible to be trapped by O₂ to form \dot{O}_2^- because of more negative potential of NH₂-MIL-125 (-0.66 eV vs. NHE) than $E^0(O_2/\dot{O}_2^-)$ (-0.33 eV vs. NHE). Additionally, the holes in the VB of TiO₂ can react with H₂O to generate •OH because the E_{VB} of TiO₂ (2.91 eV vs. NHE) is more positive compared with $E^0(H_2O/\dot{O}H)$ (2.40 eV vs. NHE). Thus, the generated •O₂⁻ and •OH subsequently took part in the CIP degradation process. In this case, lanthanum metal ions could be reduced by accepting the photo-generated

electrons and deposited around the NH₂-MIL-125, which can further be confirmed by an HRTEM imaging (not provided in this work). Also, the charge migration at the TiO₂NW/NH₂-MIL-125 interface can be verified by Bader charge simulation, indicating the Z-scheme charge transfer process (Zhao et al., 2021). Evidently, $\cdot\text{O}_2^-$ and $\cdot\text{OH}$ radicals are the main active radicals in the photodegradation process, showing strong reduction and oxidation capability respectively. Various intermediates can be formed prior to the complete mineralization into carbon dioxide and water.

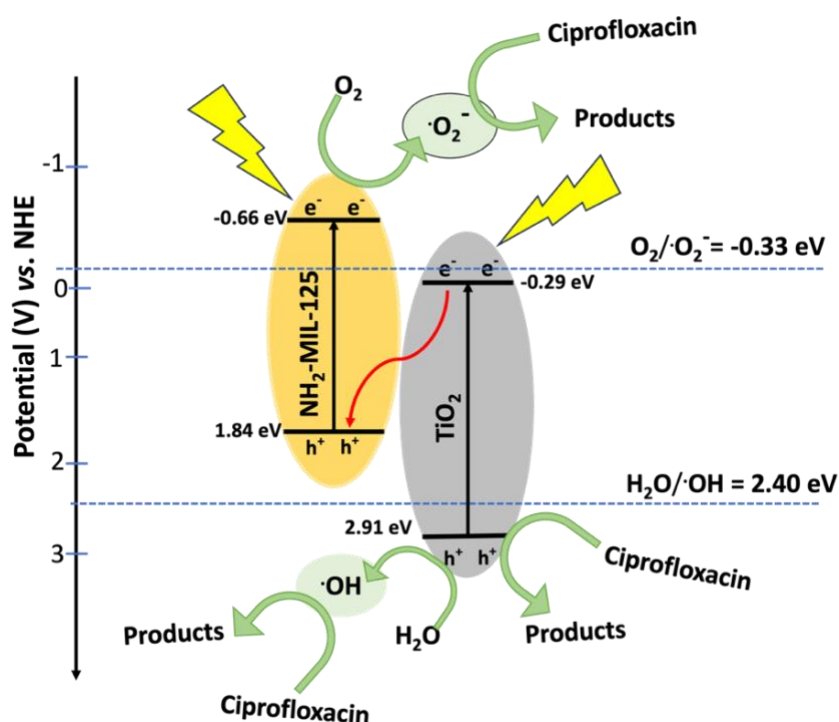


Figure 22: Proposed Z-Scheme heterojunction of TiO₂/NH₂-MIL-125 nanocomposite

Chapter 4: Conclusions and Outlook

In this research, the development and application of Metal-Organic Frameworks (MOFs)-based nanocomposites for the photocatalytic removal of Ciprofloxacin (CIP), pharmaceutical contaminants, has been demonstrated. The successful synthesis of these photocatalysts has been corroborated by structural, textural, and spectroscopic characterization techniques such as X-ray diffraction (XRD), scanning electron microscopy (SEM), and Fourier Transform Infrared Spectroscopy (FTIR).

The assessment of the photocatalytic degradation of CIP involved the use of TiO₂ nanowires (NW), pure MOF (NHM), MOF composite (TNHM), and various La-doped TNHM compositions. Remarkably, LaTNHM30 displayed the highest degradation rate at 42.7% ($k = 0.0067$), outperforming other La-doped composites. While La (30%) doping resulted in lower photodegradation compared to TNHM, it demonstrated superior performance to pure NHM. These findings underscore the significant influence of varying La concentrations on the efficiency of composite photocatalysts, offering opportunities for tailored photocatalyst design for specific applications. The superior photocatalytic performance of the TiO₂/MOF photocatalyst aligns with previous studies, emphasizing the potential for improving photocatalytic efficiency through the formation of a heterojunction with an inorganic photocatalyst like TiO₂, particularly in pharmaceutical wastewater treatment.

One of the fundamental aspects of this study involves the elucidation of a distinctive charge transfer configuration observed within the TNHM heterojunction. This configuration aligns with a Z-scheme charge transfer process, serving as the driving force behind the enhanced photocatalytic efficiency of the TNHM heterojunction. Under illumination, photo-generated electrons from the conduction band (CB) of TiO₂ NW are effectively transferred into the highest occupied molecular orbital (HOMO) of NH₂-MIL-125, facilitated by strong electrostatic attraction. This separation of electron-hole pairs between TiO₂ NW and NH₂-MIL-125 enhances the efficacy of charge separation, leading to the generation of ($\cdot\text{O}_2^-$) and ($\cdot\text{OH}$) as primary active species in the CIP degradation process. These species demonstrate substantial reduction and oxidation

capabilities, contributing to the formation of various intermediates (products) and ultimately culminating in the complete mineralization of CIP to carbon dioxide and water.

It is essential to acknowledge the limitations of the experimental setup as a potential factor contributing to these results. Moreover, the scarcity of existing literature on Lanthanum as a doping metal in MOFs raises questions about its mechanism of impact, particularly considering the potential role of Lanthanum compounds in the doping effect. This result invites further exploration into the unique aspects of Lanthanum doping within the context of MOFs-based photocatalysis.

In conclusion, this research makes a significant contribution to the field of photocatalytic removal of pharmaceutical contaminants, with a specific emphasis on addressing the persistence of CIP. The novel utilization of MOFs-based nanocomposites, especially the $\text{TiO}_2\text{NW}/\text{NH}_2\text{-MIL-125}$ composite, exhibits remarkable potential for enhancing the degradation of antibiotics in water. The elucidated mechanism provides a strong foundation for further advancements in this field and the development of more efficient photocatalytic materials. There is a clear need for progress in both the preparation of photocatalysts and the design of photoreactors to harness the full potential of this technology.

References

- AbdulMubarak, N. S., Foo, K. Y., Schneider, R., Abdelhameed, R. M., & Sabar, S. (2022). The chemistry of MIL-125 based materials: Structure, synthesis, modification strategies and photocatalytic applications. *Journal of Environmental Chemical Engineering*, 10(1), 106883. <https://doi.org/10.1016/j.jece.2021.106883>
- Afsa, S., Sallem, O. F., Abdeljelil, N. B., Feriani, A., Najjar, M. F., & Mansour, H. B. (2021). In vivo toxicities of the hospital effluent in Mahdia Tunisia. *Journal of Water and Health*, 19(3), 499-511. <https://doi.org/10.2166/wh.2021.024>
- Ahmadpour, N., Sayadi, M. H., & Homaeigohar, S. (2020). A hierarchical Ca/TiO₂/NH₂-MIL-125 nanocomposite photocatalyst for solar visible light induced photodegradation of organic dye pollutants in water. *RSC Advances*, 10(50), 29808-29820. <https://doi.org/10.1039/D0RA05192F>
- Al Qarni, H., Collier, P., O'Keeffe, J., & Akunna, J. (2016). Investigating the removal of some pharmaceutical compounds in hospital wastewater treatment plants operating in Saudi Arabia. *Environmental Science and Pollution Research*, 23, 13003-13014. <https://doi.org/10.1007/s11356-016-6389-7>
- Alharbi, O. A., Jarvis, E., Galani, A., Thomaidis, N. S., Nika, M.-C., & Chapman, D. V. (2023). Assessment of selected pharmaceuticals in Riyadh wastewater treatment plants, Saudi Arabia: Mass loadings, seasonal variations, removal efficiency and environmental risk. *Science of The Total Environment*, 882, 163284. <https://doi.org/10.1016/j.scitotenv.2023.163284>
- Alidina, M., Hoppe-Jones, C., Yoon, M., Hamadeh, A. F., Li, D., & Drewes, J. E. (2014). The occurrence of emerging trace organic chemicals in wastewater effluents in Saudi Arabia. *Science of the Total Environment*, 478, 152-162. <https://doi.org/10.1016/j.scitotenv.2014.01.093>
- Askari, N., Beheshti, M., Mowla, D., & Farhadian, M. (2020). Fabrication of CuWO₄/Bi₂S₃/ZIF67 MOF: A novel double Z-scheme ternary heterostructure for boosting visible-light photodegradation of antibiotics. *Chemosphere*, 251, 126453. <https://doi.org/10.1016/j.chemosphere.2020.126453>

- Barzegar, M. H., Ghaedi, M., Madadi Avargani, V., Sabzehmeidani, M. M., Sadeghfard, F. & Jannesar, R. (2019). Electrochemical synthesis and efficient photocatalytic degradation of azo dye alizarin yellow R by Cu/CuO nanorods under visible LED light irradiation using experimental design methodology. *Polyhedron*, 158, 506–514. <https://doi.org/10.1016/J.POLY.2018.10.040>
- Baskar, A. V., Bolan, N., Hoang, S. A., Sooriyakumar, P., Kumar, M., Singh, L., . . . Siddique, K. H. M. (2022). Recovery, regeneration and sustainable management of spent adsorbents from wastewater treatment streams: A review. *Science of The Total Environment*, 822, 153555. <https://doi.org/10.1016/j.scitotenv.2022.153555>
- Batt, A. L., Kim, S., & Aga, D. S. (2007). Comparison of the occurrence of antibiotics in four full-scale wastewater treatment plants with varying designs and operations. *Chemosphere*, 68(3), 428-435. <https://doi.org/10.1016/j.chemosphere.2007.01.008>
- Bedia, J., Muelas-Ramos, V., Peñas-Garzón, M., Gómez-Avilés, A., Rodríguez, J. J., & Belver, C. (2019). A review on the synthesis and characterization of metal organic frameworks for photocatalytic water purification. *Catalysts*, 9(1), 52. <https://doi.org/10.3390/catal9010052>
- Benotti, M. J., Trenholm, R. A., Vanderford, B. J., Holady, J. C., Stanford, B. D., & Snyder, S. A. (2009). Pharmaceuticals and endocrine disrupting compounds in U.S. drinking water. *Environmental Science and Technology*, 43(3), 597-603. <https://doi.org/10.1021/es801845a>
- Blair, B. D., Crago, J. P., Hedman, C. J., & Klaper, R. D. (2013). Pharmaceuticals and personal care products found in the Great Lakes above concentrations of environmental concern. *Chemosphere*, 93(9), 2116-2123. <https://doi.org/10.1016/j.chemosphere.2013.07.057>
- Chang, Y., Wu, C., Wang, H., Xiong, Y., Chen, Y., Ke, K., Dong, S. (2017). Effect of post-heat treatment on the photocatalytic activity of titanium dioxide nanowire membranes deposited on a Ti substrate. *RSC Advances*, 7, 21422-21429. <https://doi.org/10.1039/C7RA02092A>
- Chen, W.-Q., Li, L.-Y., Li, L., Qiu, W.-H., Tang, L., Xu, L., Wu, M.-H. (2019). MoS₂/ZIF-8 hybrid materials for environmental catalysis: solar-driven antibiotic-degradation engineering. *Engineering*, 5(4), 755-767. <https://doi.org/10.1016/j.eng.2019.02.003>

- Chiron, S., Minero, C., & Vione, D. (2006). Photodegradation processes of the antiepileptic drug carbamazepine, relevant to estuarine waters. *Environmental Science & Technology*, 40(19), 5977-5983. <https://doi.org/10.1021/es060502y>
- Chougala, L., Yatnatti, M., Lingangoudar, R., Kamble, R., & Kadadevarmath, J. (2017). A Simple Approach on Synthesis of TiO₂ Nanoparticles and its Application in dye Sensitized Solar Cells. *Journal of Nano- and Electronic Physics*, 9, 04005-04001. [https://doi.org/10.21272/jnep.9\(4\).04005](https://doi.org/10.21272/jnep.9(4).04005)
- Cui, L., Zou, X., Liu, Y., Li, X., Jiang, L., Li, C., Wang, Y. (2020). Dramatic enhancement of photocatalytic H₂ evolution over hydrolyzed MOF-5 coupled Zn_{0.2}Cd_{0.8}S heterojunction. *Journal of Colloid and Interface Science*, 577, 233-241. <https://doi.org/10.1016/J.JCIS.2020.05.023>
- Dai, D., Qiu, J., Li, M., Xu, J., Zhang, L., & Yao, J. (2021). Construction of two-dimensional BiOI on carboxyl-rich MIL-121 for visible-light photocatalytic degradation of tetracycline. *Journal of Alloys and Compounds*, 872, 159711. <https://doi.org/10.1016/j.jallcom.2021.159711>
- de Andrade, J. R., Oliveira, M. F., da Silva, M. G. C., & Vieira, M. G. A. (2018). Adsorption of pharmaceuticals from water and wastewater using nonconventional low-cost materials: a review. *Industrial & Engineering Chemistry Research*, 57(9), 3103-3127. <https://doi.org/10.1021/acs.iecr.7b05137>
- Deo, R. P. (2014). Pharmaceuticals in the surface water of the USA: a review. *Current Environmental Health Reports*, 1, 113-122. <https://doi.org/10.1007/s40572-014-0015-y>
- Di, J., Xia, J., Ji, M., Yin, S., Li, H., Xu, H., Li, H. (2015). Controllable synthesis of Bi₄O₅Br₂ ultrathin nanosheets for photocatalytic removal of ciprofloxacin and mechanism insight. *Journal of Materials Chemistry A*, 3(29), 15108-15118. <https://doi.org/10.1039/C5TA02388B>
- Dubadi, R., Huang, S. D. & Jaroniec, M. (2023). Mechanochemical Synthesis of Nanoparticles for Potential Antimicrobial Applications. *Materials*, 16(4), 1460. <https://doi.org/10.3390/MA16041460>
- Eniola, J. O., Kumar, R., & Barakat, M. A. (2019). Adsorptive removal of antibiotics from water over natural and modified adsorbents. *Environmental Science and Pollution Research*, 26(34), 34775-34788. <https://doi.org/10.1007/s11356-019-06641-6>

- Eniola, J. O., Kumar, R., Barakat, M. A., & Rashid, J. (2022). A review on conventional and advanced hybrid technologies for pharmaceutical wastewater treatment. *Journal of Cleaner Production*, 356, 131826. <https://doi.org/https://doi.org/10.1016/j.jclepro.2022.131826>
- Fang, Y., Zhu, S.-R., Wu, M.-K., Zhao, W.-N., & Han, L. (2018). MOF-derived In₂S₃ nanorods for photocatalytic removal of dye and antibiotics. *Journal of Solid State Chemistry*, 266, 205-209. <https://doi.org/10.1016/j.jssc.2018.07.026>
- Fu, J., Yu, J., Jiang, C., & Cheng, B. (2018). g-C₃N₄-Based heterostructured photocatalysts. *Advanced Energy Materials*, 8(3), 1701503. <https://doi.org/10.1002/aenm.201701503>
- Fu, Y., Sun, D., Chen, Y., Huang, R., Ding, Z., Fu, X., & Li, Z. (2012). An Amine-Functionalized Titanium Metal–Organic Framework Photocatalyst with Visible-Light-Induced Activity for CO₂ Reduction. *Angewandte Chemie International Edition*, 51(14), 3364-3367. <https://doi.org/https://doi.org/10.1002/anie.201108357>
- Fu, Y., Zhang, K., Zhang, Y., Cong, Y., & Wang, Q. (2021). Fabrication of visible-light-active MR/NH₂-MIL-125(Ti) homojunction with boosted photocatalytic performance. *Chemical Engineering Journal*, 412, 128722-128722. <https://doi.org/10.1016/J.CEJ.2021.128722>
- Gong, Y.-N., Mei, J.-H., Liu, J.-W., Huang, H.-H., Zhang, J.-H., Li, X., Lu, T.-B. (2021). Manipulating metal oxidation state over ultrastable metal-organic frameworks for boosting photocatalysis. *Applied Catalysis B: Environmental*, 292, 120156-120156. <https://doi.org/10.1016/j.apcatb.2021.120156>
- Gong, Y. N., Mei, J. H., Liu, J. W., Huang, H. H., Zhang, J. H., Li, X., Lu, T. B. (2021). Manipulating metal oxidation state over ultrastable metal-organic frameworks for boosting photocatalysis. *Applied Catalysis B: Environmental*, 292, 120156-120156. <https://doi.org/10.1016/J.APCATB.2021.120156>
- Hendon, C. H., Tiana, D., Fontecave, M., Sanchez, C., D'arras, L., Sassoey, C., Walsh, A. (2013). Engineering the Optical Response of the Titanium-MIL-125 Metal–Organic Framework through Ligand Functionalization. *Journal of the American Chemical Society*, 135(30), 10942-10945. <https://doi.org/10.1021/ja405350u>

- Hontela, A., & Habibi, H. R. (2013). 8 - Personal Care Products in the Aquatic Environment: A Case Study on the Effects of Triclosan in Fish. In K. B. Tierney, A. P. Farrell, & C. J. Brauner (Eds.), *Fish Physiology* (Vol. 33, pp. 411-437). Academic Press. <https://doi.org/10.1016/B978-0-12-398254-4.00008-X>
- Howarth, A. J., Peters, A. W., Vermeulen, N. A., Wang, T. C., Hupp, J. T., & Farha, O. K. (2017). Best practices for the synthesis, activation, and characterization of metal–organic frameworks. *Chemistry of Materials*, 29(1), 26-39. <https://doi.org/10.1021/acs.chemmater.6b02626>
- Huang, C., Wang, J., Li, M., Lei, X., & Wu, Q. (2021). Construction of a novel Z-scheme V2O5/NH2-MIL-101(Fe) composite photocatalyst with enhanced photocatalytic degradation of tetracycline. *Solid State Sciences*, 117, 106611. <https://doi.org/10.1016/j.solidstatesciences.2021.106611>
- Huang, Q., Hu, Y., Pei, Y., Zhang, J., & Fu, M. (2019). In situ synthesis of TiO2@NH2-MIL-125 composites for use in combined adsorption and photocatalytic degradation of formaldehyde. *Applied Catalysis B: Environmental*, 259, 118106-118106. <https://doi.org/10.1016/j.apcatb.2019.118106>
- Ikreedeegh, R. R., & Tahir, M. (2021). A critical review in recent developments of metal-organic-frameworks (MOFs) with band engineering alteration for photocatalytic CO2 reduction to solar fuels. *Journal of CO2 Utilization*, 43, 101381-101381. <https://doi.org/10.1016/j.jcou.2020.101381>
- Ikreedeegh, R. R., & Tahir, M. (2023). Ternary nanocomposite of NH2-MIL-125 (Ti) MOF-modified TiO2 nanotube arrays (TNTs) with GO electron mediator for enhanced photocatalytic conversion of CO2 to solar fuels under visible light. *Journal of Alloys and Compounds*, 172465. <https://doi.org/10.1016/j.jallcom.2023.172465>
- Islam, M. J., Kim, H. K., Reddy, D. A., Kim, Y., Ma, R., Baek, H., Kim, T. K. (2017). Hierarchical BiOI nanostructures supported on a metal organic framework as efficient photocatalysts for degradation of organic pollutants in water. *Dalton Transactions*, 46(18), 6013-6023. <https://doi.org/10.1039/C7DT00459A>
- Jafari, M., Vanoppen, M., van Agtmaal, J. M. C., Cornelissen, E. R., Vrouwenvelder, J. S., Verliefde, A., Picioreanu, C. (2021). Cost of fouling in full-scale reverse osmosis and nanofiltration installations in the Netherlands. *Desalination*, 500, 114865. <https://doi.org/10.1016/j.desal.2020.114865>

- Jarusheh, H. S., Yusuf, A., Banat, F., Haija, M. A., & Palmisano, G. (2022). Integrated photocatalytic technologies in water treatment using ferrites nanoparticles. *Journal of Environmental Chemical Engineering*, 108204. <https://doi.org/10.1016/j.jece.2022.108204>
- Jiménez-Bambague, E. M., Madera-Parra, C. A., Ortiz-Escobar, A. C., Morales-Acosta, P. A., Peña-Salamanca, E. J., & Machuca-Martínez, F. (2020). High-rate algal pond for removal of pharmaceutical compounds from urban domestic wastewater under tropical conditions. Case study: Santiago de Cali, Colombia. *Water Science and Technology*, 82(6), 1031-1043. <https://doi.org/10.2166/WST.2020.362>
- Jin, C., Wang, M., Li, Z., Kang, J., Zhao, Y., Han, J., & Wu, Z. (2020). Two dimensional Co₃O₄/g-C₃N₄ Z-scheme heterojunction: Mechanism insight into enhanced peroxymonosulfate-mediated visible light photocatalytic performance. *Chemical Engineering Journal*, 398, 125569. <https://doi.org/10.1016/j.cej.2020.125569>
- Kagle, J., Porter, A. W., Murdoch, R. W., Rivera-Cancel, G., & Hay, A. G. (2009). Biodegradation of pharmaceutical and personal care products. *Advances in Applied Microbiology*, 67, 65-108. [https://doi.org/10.1016/S0065-2164\(08\)01003-4](https://doi.org/10.1016/S0065-2164(08)01003-4)
- Kavitha, V. (2022). Global prevalence and visible light mediated photodegradation of pharmaceuticals and personal care products (PPCPs)-a review. *Results in Engineering*, 14, 100469-100469. <https://doi.org/10.1016/J.RINENG.2022.100469>
- Khanzada, N. K., Farid, M. U., Kharraz, J. A., Choi, J., Tang, C. Y., Nghiem, L. D., . . . An, A. K. (2020). Removal of organic micropollutants using advanced membrane-based water and wastewater treatment: A review. *Journal of Membrane Science*, 598, 117672. <https://doi.org/10.1016/j.memsci.2019.117672>
- Krishnan, R., Shibu, S. N., Poelman, D., Badyal, A. K., Kunti, A. K., Swart, H. C. & Menon, S. G. (2022). Recent advances in microwave synthesis for photoluminescence and photocatalysis. *Materials Today Communications*, 32, 103890. <https://doi.org/10.1016/J.MTCOMM.2022.103890>
- Kumar, M., Jaiswal, S., Sodhi, K. K., Shree, P., Singh, D. K., Agrawal, P. K., & Shukla, P. (2019). Antibiotics bioremediation: Perspectives on its ecotoxicity and resistance. *Environment International*, 124, 448-461. <https://doi.org/10.1016/J.ENVINT.2018.12.065>

- Kumar, R., Qureshi, M., Vishwakarma, D. K., Al-Ansari, N., Kuriqi, A., Elbeltagi, A., & Saraswat, A. (2022). A review on emerging water contaminants and the application of sustainable removal technologies. *Case Studies in Chemical and Environmental Engineering*, 6, 100219-100219.
<https://doi.org/10.1016/J.CSCEE.2022.100219>
- Lai, C., Zhang, M., Li, B., Huang, D., Zeng, G., Qin, L., Li, L. (2019). Fabrication of CuS/BiVO₄ (0 4 0) binary heterojunction photocatalysts with enhanced photocatalytic activity for Ciprofloxacin degradation and mechanism insight. *Chemical Engineering Journal*, 358, 891-902.
<https://doi.org/10.1016/j.cej.2018.10.072>
- Lajeunesse, A., Smyth, S. A., Barclay, K., Sauvé, S., & Gagnon, C. (2012). Distribution of antidepressant residues in wastewater and biosolids following different treatment processes by municipal wastewater treatment plants in Canada. *Water Research*, 46(17), 5600-5612.
<https://doi.org/10.1016/J.WATRES.2012.07.042>
- Le, V. T., Tran, V. A., Tran, D. L., Nguyen, T. L. H., & Doan, V.-D. (2021). Fabrication of Fe₃O₄/CuO@C composite from MOF-based materials as an efficient and magnetically separable photocatalyst for degradation of ciprofloxacin antibiotic. *Chemosphere*, 270, 129417.
<https://doi.org/doi.org/10.1016/j.chemosphere.2020.129417>
- Lesho, E. P., & Laguio-Vila, M. (2019). The Slow-Motion Catastrophe of Antimicrobial Resistance and Practical Interventions for All Prescribers. *Mayo Clinic Proceedings*, 94(6), 1040-1047.
<https://doi.org/10.1016/j.mayocp.2018.11.005>
- Lin, B., Li, S., Peng, Y., Chen, Z., & Wang, X. (2021). MOF-derived core/shell C-TiO₂/CoTiO₃ type II heterojunction for efficient photocatalytic removal of antibiotics. *Journal of Hazardous Materials*, 406, 124675-124675.
<https://doi.org/10.1016/J.JHAZMAT.2020.124675>
- Liu, Y., Ding, S., Shi, Y., Liu, X., Wu, Z., Jiang, Q., . . . Hu, J. (2018). Construction of CdS/CoOx core-shell nanorods for efficient photocatalytic H₂ evolution. *Applied Catalysis B: Environmental*, 234, 109-116.
<https://doi.org/10.1016/j.apcatb.2018.04.037>
- Low, J., Yu, J., Jaroniec, M., Wageh, S., Al-Ghamdi J X Low, A. A., Yu, J. G., . . . Jaroniec, M. (2017). Heterojunction photocatalysts. *Wiley Online Library*, 29(20). <https://doi.org/10.1002/adma.201601694>

- Lu, J., Hao, H., Zhang, L., Xu, Z., Zhong, L., Zhao, Y., . . . Pu, H. (2018). The investigation of the role of basic lanthanum (La) species on the improvement of catalytic activity and stability of HZSM-5 material for eliminating methanethiol-(CH₃SH). *Applied Catalysis B: Environmental*, 237, 185-197. <https://doi.org/10.1016/j.apcatb.2018.05.063>
- Lu, N., Wang, P., Su, Y., Yu, H., Liu, N., & Quan, X. (2019). Construction of Z-Scheme g-C₃N₄/RGO/WO₃ with in situ photoreduced graphene oxide as electron mediator for efficient photocatalytic degradation of ciprofloxacin. *Chemosphere*, 215, 444-453. <https://doi.org/10.1016/j.chemosphere.2018.10.065>
- Ly, S. W., Cong, Y., Chen, X., Wang, W., & Che, L. (2021). Developing fine-tuned metal–organic frameworks for photocatalytic treatment of wastewater: A review. *Chemical Engineering Journal*, 133605-133605. <https://doi.org/10.1016/J.CEJ.2021.133605>
- Ma, Y., Chen, Z., Qu, D., & Shi, J. (2016). Synthesis of chemically bonded BiOCl@Bi₂WO₆ microspheres with exposed (0 2 0) Bi₂WO₆ facets and their enhanced photocatalytic activities under visible light irradiation. *Applied Surface Science*, 361, 63-71. <https://doi.org/10.1016/j.apsusc.2015.11.130>
- Mackuľak, T., Ćernanský, S., Fehér, M., Birošová, L., & Gál, M. (2019). Pharmaceuticals, drugs, and resistant microorganisms—environmental impact on population health. *Current Opinion in Environmental Science & Health*, 9, 40-48. <https://doi.org/10.1016/j.coesh.2019.04.002>
- Maimaitizi, H., Abulizi, A., Kadeer, K., Talifu, D., & Tursun, Y. (2020). In situ synthesis of Pt and N co-doped hollow hierarchical BiOCl microsphere as an efficient photocatalyst for organic pollutant degradation and photocatalytic CO₂ reduction. *Applied Surface Science*, 502, 144083. <https://doi.org/10.1016/j.apsusc.2019.144083>
- Majumder, S., Chatterjee, S., Basnet, P., & Mukherjee, J. (2020). ZnO based nanomaterials for photocatalytic degradation of aqueous pharmaceutical waste solutions – A contemporary review. *Environmental Nanotechnology, Monitoring & Management*, 14, 100386-100386. <https://doi.org/10.1016/J.ENMM.2020.100386>

- Mamta, Bhushan, S., Rana, M. S., Raychaudhuri, S., Simsek, H., & Prajapati, S. K. (2020). Algae- and bacteria-driven technologies for pharmaceutical remediation in wastewater. Removal of Toxic Pollutants through Microbiological and Tertiary Treatment: New Perspectives, 373-408. <https://doi.org/10.1016/B978-0-12-821014-7.00015-0>
- Metcalf, C. D., Chu, S., Judt, C., Li, H., Oakes, K. D., Servos, M. R., & Andrews, D. M. (2010). Antidepressants and their metabolites in municipal wastewater, and downstream exposure in an urban watershed. *Environmental Toxicology and Chemistry*, 29(1), 79-89. <https://doi.org/10.1002/ETC.27>
- Milaković, M., Vestergaard, G., González-Plaza, J. J., Petrić, I., Šimatović, A., Senta, I., Udiković-Kolić, N. (2019). Pollution from azithromycin-manufacturing promotes macrolide-resistance gene propagation and induces spatial and seasonal bacterial community shifts in receiving river sediments. *Environment international*, 123, 501-511. <https://doi.org/10.1016/j.envint.2018.12.050>
- Muelas-Ramos, V., Belver, C., Rodriguez, J. J., & Bedia, J. (2021). Synthesis of noble metal-decorated NH₂-MIL-125 titanium MOF for the photocatalytic degradation of acetaminophen under solar irradiation. *Separation and Purification Technology*, 272, 118896. <https://doi.org/10.1016/j.seppur.2021.118896>
- Muelas-Ramos, V., Sampaio, M., Silva, C., Bedia, J., Rodríguez, J., Faria, J., & Belver, C. (2021). Degradation of diclofenac in water under LED irradiation using combined g-C₃N₄/NH₂-MIL-125 photocatalysts. *Journal of Hazardous Materials*, 126199. <https://doi.org/10.1016/j.jhazmat.2021.126199>
- Mumtaz, N., Javaid, A., Imran, M., Latif, S., Hussain, N., Nawaz, S., & Bilal, M. (2022). Nanoengineered metal-organic framework for adsorptive and photocatalytic mitigation of pharmaceuticals and pesticide from wastewater. *Environmental Pollution*, 308, 119690. <https://doi.org/10.1016/j.envpol.2022.119690>
- Nas, B., Dolu, T., & Koyuncu, S. (2021). Behavior and Removal of Ciprofloxacin and Sulfamethoxazole Antibiotics in Three Different Types of Full-Scale Wastewater Treatment Plants: A Comparative Study. *Water, Air, & Soil Pollution*, 232(4), 127. <https://doi.org/10.1007/s11270-021-05067-6>
- Naushad, M., Sharma, G., & Alothman, Z. A. (2019). Photodegradation of toxic dye using Gum Arabic-crosslinked-poly (acrylamide)/Ni (OH)₂/FeOOH nanocomposites hydrogel. *Journal of Cleaner Production*, 241, 118263. <https://doi.org/10.1016/j.jclepro.2019.118263>

- Nguyen, V.-H., & Wu, J. C. S. (2018). Recent developments in the design of photoreactors for solar energy conversion from water splitting and CO₂ reduction. *Applied Catalysis A: General*, 550, 122-141. <https://doi.org/https://doi.org/10.1016/j.apcata.2017.11.002>
- Nkoh, J. N., Oderinde, O., Etafo, N. O., Kifle, G. A., Okeke, E. S., Ejeromedoghene, O., . . . Oladeji, O. S. (2023). Recent perspective of antibiotics remediation: A review of the principles, mechanisms, and chemistry controlling remediation from aqueous media. *Science of The Total Environment*, 881, 163469. <https://doi.org/10.1016/j.scitotenv.2023.163469>
- Nunes, D., Pimentel, A., Santos, L., Barquinha, P., Pereira, L., Fortunato, E. & Martins, R. (2019). Synthesis, design, and morphology of metal oxide nanostructures. In *Metal Oxide Nanostructures* (pp. 21–57). Elsevier. <https://doi.org/10.1016/B978-0-12-811512-1.00002-3>
- Ong, W.-J., Tan, L.-L., Ng, Y. H., Yong, S.-T., & Chai, S.-P. (2016). Graphitic Carbon Nitride (g-C₃N₄)-Based Photocatalysts for Artificial Photosynthesis and Environmental Remediation: Are We a Step Closer To Achieving Sustainability? *Chemical Reviews*, 116(12), 7159-7329. <https://doi.org/10.1021/acs.chemrev.6b00075>
- Palmisano, G., Augugliaro, V., Pagliaro, M., & Palmisano, L. (2007). Photocatalysis: a promising route for 21st century organic chemistry. *Chemical Communications*(33), 3425-3437. <https://doi.org/10.1039/B700395C>
- Phoon, B. L., Ong, C. C., Saheed, M. S. M., Show, P.-L., Chang, J.-S., Ling, T. C., . . . Juan, J. C. (2020). Conventional and emerging technologies for removal of antibiotics from wastewater. *Journal of Hazardous Materials*, 400, 122961. <https://doi.org/10.1016/j.jhazmat.2020.122961>
- Qi, K., Zhuang, C., Zhang, M., Gholami, P. & Khataee, A. (2022). Sonochemical synthesis of photocatalysts and their applications. *Journal of Materials Science & Technology*, 123, 243–256. <https://doi.org/10.1016/J.JMST.2022.02.019>
- Qin, X., Qiang, T., Chen, L., & Wang, S. (2021). Construction of 3D N-CQD/MOF-5 photocatalyst to improve the photocatalytic performance of MOF-5 by changing the electron transfer path. *Microporous and Mesoporous Materials*, 315, 110889-110889. <https://doi.org/10.1016/J.MICROMESO.2021.110889>
- Quan, X., Tan, H., Zhao, Q., & Sang, X. (2007). Preparation of lanthanum-doped TiO₂ photocatalysts by coprecipitation. *Journal of Materials Science*, 42, 6287-6296. <https://doi.org/10.1007/s10853-006-1022-7>

- Ramírez-Durán, N., Moreno-Pérez, P. A., & Sandoval-Trujillo, A. H. (2019). Bacterial Treatment of Pharmaceutical Industry Effluents. *Ecopharmacovigilance: Multidisciplinary Approaches to Environmental Safety of Medicines*, 175-187. https://doi.org/10.1007/698_2017_167
- Raptopoulou, C. P. (2021). Metal-Organic Frameworks: Synthetic Methods and Potential Applications. *Materials*, 14(2), 1–32. <https://doi.org/10.3390/MA14020310>
- Rathi, B. S., Kumar, P. S., & Show, P.-L. (2021). A review on effective removal of emerging contaminants from aquatic systems: Current trends and scope for further research. *Journal of Hazardous Materials*, 409, 124413. <https://doi.org/10.1016/j.jhazmat.2020.124413>
- Ren, G., Han, H., Wang, Y., Liu, S., Zhao, J., Meng, X., & Li, Z. (2021). Recent Advances of Photocatalytic Application in Water Treatment: A Review. *Nanomaterials* 2021, Vol. 11, Page 1804, 11(7), 1804-1804. <https://doi.org/10.3390/NANO11071804>
- Rozman, D., Hrkál, Z., Váňa, M., Vymazal, J., & Boukalová, Z. (2017). Occurrence of pharmaceuticals in wastewater and their interaction with shallow aquifers: a case study of Horní Beřkovice, Czech Republic. *Water*, 9(3), 218. <https://doi.org/10.1016/j.jhazmat.2020.124413>
- Safaralizadeh, E., Mahjoub, A. R., Fazlali, F., & Bagheri, H. (2021). Facile construction of C₃N₄-TE@TiO₂/UiO-66 with double Z-scheme structure as high performance photocatalyst for degradation of tetracycline. *Ceramics International*, 47(2), 2374-2387. <https://doi.org/j.ceramint.2020.09.080>
- Samal, K., Mahapatra, S., & Ali, M. H. (2022). Pharmaceutical wastewater as Emerging Contaminants (EC): Treatment technologies, impact on environment and human health. *Energy Nexus*, 100076. <https://doi.org/10.1016/j.nexus.2022.100076>
- Shah, A., & Shah, M. (2020). Characterisation and bioremediation of wastewater: a review exploring bioremediation as a sustainable technique for pharmaceutical wastewater. *Groundwater for Sustainable Development*, 11, 100383. <https://doi.org/10.1016/j.gsd.2020.100383>
- Shanableh, A., Semreen, M., Semerjian, L., Abdallah, M., Mousa, M., Darwish, N., & Baalbaki, Z. (2019). Contaminants of emerging concern in Sharjah wastewater treatment plant, Sharjah, UAE. 14(4), 225-234. <https://doi.org/10.1680/JENES.18.00029>

- Sheng, Y., Yi, D., Qingsong, H., Ting, W., Ming, L., Yong, C., Xia, J. (2019). CQDs modified PbBiO₂Cl nanosheets with improved molecular oxygen activation ability for photodegradation of organic contaminants. *Journal of Photochemistry and Photobiology A: Chemistry*, 382, 111921. <https://doi.org/10.1016/j.jphotochem.2019.111921>
- Shraim, A., Diab, A., Alsuhaime, A., Niazy, E., Metwally, M., Amad, M., Dawoud, A. (2017). Analysis of some pharmaceuticals in municipal wastewater of Almadinah Almunawarah. *Arabian Journal of Chemistry*, 10, S719-S729. <https://doi.org/10.1016/j.arabjc.2012.11.014>
- Skouteris, G., Rodriguez-Garcia, G., Reinecke, S. F., & Hampel, U. (2020). The use of pure oxygen for aeration in aerobic wastewater treatment: A review of its potential and limitations. *Bioresource technology*, 312, 123595. <https://doi.org/10.1016/j.biortech.2020.123595>
- Sohrabnezhad, S., Pourahmad, A., & Karimi, M. F. (2020). Magnetite-metal organic framework core@shell for degradation of ampicillin antibiotic in aqueous solution. *Journal of Solid State Chemistry*, 288, 121420. <https://doi.org/10.1016/j.jssc.2020.121420>
- Song, H., Sun, Z., Xu, Y., Han, Y., Xu, J., Wu, J., . . . Zhang, X. (2019). Fabrication of NH₂-MIL-125 (Ti) incorporated TiO₂ nanotube arrays composite anodes for highly efficient PEC water splitting. *Separation and Purification Technology*, 228, 115764. <https://doi.org/10.1016/j.seppur.2019.115764>
- Stuart, M., Lapworth, D., Crane, E., & Hart, A. (2012). Review of risk from potential emerging contaminants in UK groundwater. *Science of The Total Environment*, 416, 1-21. <https://doi.org/10.1016/J.SCITOTENV.2011.11.072>
- Swetha, S., Janani, B., & Khan, S. S. (2022). A critical review on the development of metal-organic frameworks for boosting photocatalysis in the fields of energy and environment. *Journal of Cleaner Production*, 333, 130164-130164. <https://doi.org/10.1016/J.JCLEPRO.2021.130164>
- Tahir, M., Ajiwokewu, B., Bankole, A. A., Ismail, O., Al-Amodi, H., & Kumar, N. (2023). MOF based composites with engineering aspects and morphological developments for photocatalytic CO₂ reduction and hydrogen production: A comprehensive review. *Journal of Environmental Chemical Engineering*, 109408. <https://doi.org/10.1016/j.jece.2023.109408>

- Tiwari, B., Sellamuthu, B., Ouarda, Y., Drogui, P., Tyagi, R. D., & Buelna, G. (2017). Review on fate and mechanism of removal of pharmaceutical pollutants from wastewater using biological approach. *Bioresource Technology*, 224, 1-12. <https://doi.org/10.1016/J.BIORTECH.2016.11.042>
- Tran, N. H., Li, J., Hu, J., & Ong, S. L. (2014). Occurrence and suitability of pharmaceuticals and personal care products as molecular markers for raw wastewater contamination in surface water and groundwater. *Environmental Science and Pollution Research*, 21, 4727-4740. <https://doi.org/10.1007/s11356-013-2428-9>
- Walton, K. S., & Snurr, R. Q. (2007). Applicability of the BET method for determining surface areas of microporous metal– organic frameworks. *Journal of the American Chemical Society*, 129(27), 8552-8556. <https://doi.org/10.1021/ja071174k>
- Wan, S., Ou, M., Zhong, Q., & Wang, X. (2019). Perovskite-type CsPbBr₃ quantum dots/Uio-66(NH₂) nanojunction as efficient visible-light-driven photocatalyst for CO₂ reduction. *Chemical Engineering Journal*, 358, 1287-1295. <https://doi.org/10.1016/J.CEJ.2018.10.120>
- Wang, B., Liu, G., Ye, B., Ye, Y., Zhu, W., Yin, S., Li, H. (2019). Novel CNT/PbBiO₂Br hybrid materials with enhanced broad spectrum photocatalytic activity toward ciprofloxacin (CIP) degradation. *Journal of Photochemistry and Photobiology A: Chemistry*, 382, 111901. <https://doi.org/10.1016/j.jphotochem.2019.111901>
- Wang, C. C., Wang, X., & Liu, W. (2020). The synthesis strategies and photocatalytic performances of TiO₂/MOFs composites: A state-of-the-art review. *Chemical Engineering Journal*, 391, 123601-123601. <https://doi.org/10.1016/J.CEJ.2019.123601>
- Wang, D., Li, H., Han, Q., Jiang, W., Liu, C., & Che, G. (2021). Optimized design of BiVO₄/NH₂-MIL-53 (Fe) heterostructure for enhanced photocatalytic degradation of methylene blue and ciprofloxacin under visible light. *Journal of Physics and Chemistry of Solids*, 154, 110027. <https://doi.org/10.1016/j.jpcs.2021.110027>
- Wang, Q., Gao, Q., Al-Enizi, A. M., Nafady, A., & Ma, S. (2020). Recent advances in MOF-based photocatalysis: environmental remediation under visible light. *Inorg. Chem. Front*, 7, 300-300. <https://doi.org/10.1039/c9qi01120j>

- Wang, S., Yang, X., Zhang, X., Ding, X., Yang, Z., Dai, K., & Chen, H. (2017). A plate-on-plate sandwiched Z-scheme heterojunction photocatalyst: BiOBr-Bi₂MoO₆ with enhanced photocatalytic performance. *Applied Surface Science*, 391, 194-201. <https://doi.org/10.1016/j.apsusc.2016.07.070>
- Wankhade, V., Gaikwad, G. S., Dhonde, M. G., Khaty, N. T., & Thakare, S. R. (2013). Removal of organic pollutant from water by heterogenous photocatalysis: a review. *Research Journal of Chemistry and Environment*, 17, 84-94. WOS:000312896300014
- Wen, X.-J., Niu, C.-G., Zhang, L., Liang, C., Guo, H., & Zeng, G.-M. (2018). Photocatalytic degradation of ciprofloxacin by a novel Z-scheme CeO₂-Ag/AgBr photocatalyst: influencing factors, possible degradation pathways, and mechanism insight. *Journal of catalysis*, 358, 141-154. <https://doi.org/10.1016/j.jcat.2017.11.029>
- Wen, Y., Zhang, P., Sharma, V. K., Ma, X., & Zhou, H. C. (2021). Metal-organic frameworks for environmental applications. *Cell Reports Physical Science*, 2(2). <https://doi.org/10.1016/J.XCRP.2021.100348>
- Xia, T., Lin, Y., Li, W., & Ju, M. (2021). Photocatalytic degradation of organic pollutants by MOFs based materials: A review. *Chinese Chemical Letters*, 32(10), 2975-2984. <https://doi.org/10.1016/J.CCLET.2021.02.058>
- Xu, A.-W., Gao, Y., & Liu, H.-Q. (2002). The preparation, characterization, and their photocatalytic activities of rare-earth-doped TiO₂ nanoparticles. *Journal of Catalysis*, 207(2), 151-157. <https://doi.org/10.1006/jcat.2002.3539>
- Yan, D., Hu, H., Gao, N., Ye, J., & Ou, H. (2019). Fabrication of carbon nanotube functionalized MIL-101(Fe) for enhanced visible-light photocatalysis of ciprofloxacin in aqueous solution. *Applied Surface Science*, 498, 143836-143836. <https://doi.org/10.1016/J.APSUSC.2019.143836>
- Yuan, X., Qu, S., Huang, X., Xue, X., Yuan, C., Wang, S., Cai, P. (2021). Design of core-shelled g-C₃N₄@ZIF-8 photocatalyst with enhanced tetracycline adsorption for boosting photocatalytic degradation. *Chemical Engineering Journal*, 416, 129148. <https://doi.org/10.1016/j.cej.2021.129148>
- Zhang, B., Zhang, J., Tan, X., Shao, D., Shi, J., Zheng, L., Han, B. (2018). MIL-125-NH₂@TiO₂ Core-Shell Particles Produced by a Post-Solvothermal Route for High-Performance Photocatalytic H₂ Production. *ACS Applied Materials and Interfaces*, 10(19), 16418-16423. <https://doi.org/10.1021/ACSAMI.8B01462>

- Zhang, J., Li, Z., Qi, X.-L., & Wang, D.-Y. (2020). Recent Progress on Metal–Organic Framework and Its Derivatives as Novel Fire Retardants to Polymeric Materials. *Nano-Micro Letters*, 12(1), 173. <https://doi.org/10.1007/s40820-020-00497-z>
- Zhang, L., Cui, P., Yang, H., Chen, J., Xiao, F., Guo, Y., Liu, B. (2016). Metal–organic frameworks as promising photosensitizers for photoelectrochemical water splitting. *Advanced Science*, 3(1), 1500243. <https://doi.org/10.1002/advs.201500243>
- Zhang, Q.-Q., Ying, G.-G., Pan, C.-G., Liu, Y.-S., & Zhao, J.-L. (2015). Comprehensive evaluation of antibiotics emission and fate in the river basins of China: source analysis, multimedia modeling, and linkage to bacterial resistance. *Environmental Science & Technology*, 49(11), 6772-6782. <https://doi.org/10.1021/acs.est.5b00729>
- Zhang, S., Wang, J., Zhang, Y., Ma, J., Huang, L., Yu, S., Wang, X. (2021). Applications of water-stable metal-organic frameworks in the removal of water pollutants: A review. *Environmental Pollution*, 291, 118076-118076. <https://doi.org/10.1016/J.ENVPOL.2021.118076>
- Zhang, T., & Lin, W. (2014). Metal–organic frameworks for artificial photosynthesis and photocatalysis. *Chemical Society Reviews*, 43(16), 5982-5993. <https://doi.org/10.1039/C4CS00103F>
- Zhang, Y. X., Li, G. H., Jin, Y. X., Zhang, Y., Zhang, J., & Zhang, L. D. (2002). Hydrothermal synthesis and photoluminescence of TiO₂ nanowires. *Chemical Physics Letters*, 365(3), 300-304. [https://doi.org/10.1016/S0009-2614\(02\)01499-9](https://doi.org/10.1016/S0009-2614(02)01499-9)
- Zhao, C., Li, Y., Chu, H., Pan, X., Ling, L., Wang, P., Wang, Z. (2021). Construction of direct Z-scheme Bi₅O₇I/UiO-66-NH₂ heterojunction photocatalysts for enhanced degradation of ciprofloxacin: Mechanism insight, pathway analysis and toxicity evaluation. *Journal of Hazardous Materials*, 419, 126466. <https://doi.org/10.1016/j.jhazmat.2021.126466>
- Zhao, Y., Cai, W., Chen, J., Miao, Y., & Bu, Y. (2019). A Highly Efficient Composite Catalyst Constructed From NH₂-MIL-125(Ti) and Reduced Graphene Oxide for CO₂ Photoreduction [Original Research]. *Frontiers in Chemistry*, 7. <https://doi.org/10.3389/fchem.2019.00789>

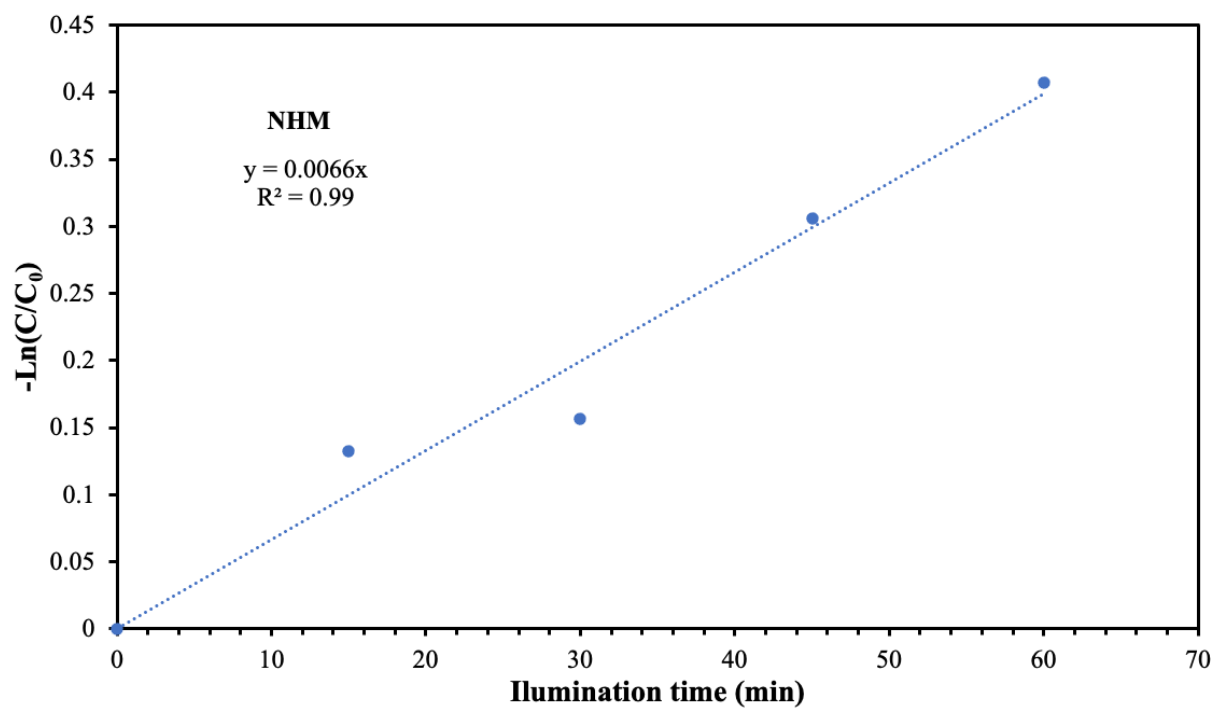
- Zhou, P., Su, C., Li, B., & Qian, Y. (2006). Treatment of high-strength pharmaceutical wastewater and removal of antibiotics in anaerobic and aerobic biological treatment processes. *Journal of Environmental Engineering*, 132(1), 129-136. [https://doi.org/10.1061/\(ASCE\)0733-9372\(2006\)132:1\(129\)](https://doi.org/10.1061/(ASCE)0733-9372(2006)132:1(129))
- Zhu, W., Zhang, C., Li, Q., Xiong, L., Chen, R., Wan, X., . . . Peng, Y. (2018). Selective reduction of CO₂ by conductive MOF nanosheets as an efficient co-catalyst under visible light illumination. *Applied Catalysis B: Environmental*, 238, 339-345. <https://doi.org/10.1016/J.APCATB.2018.07.024>

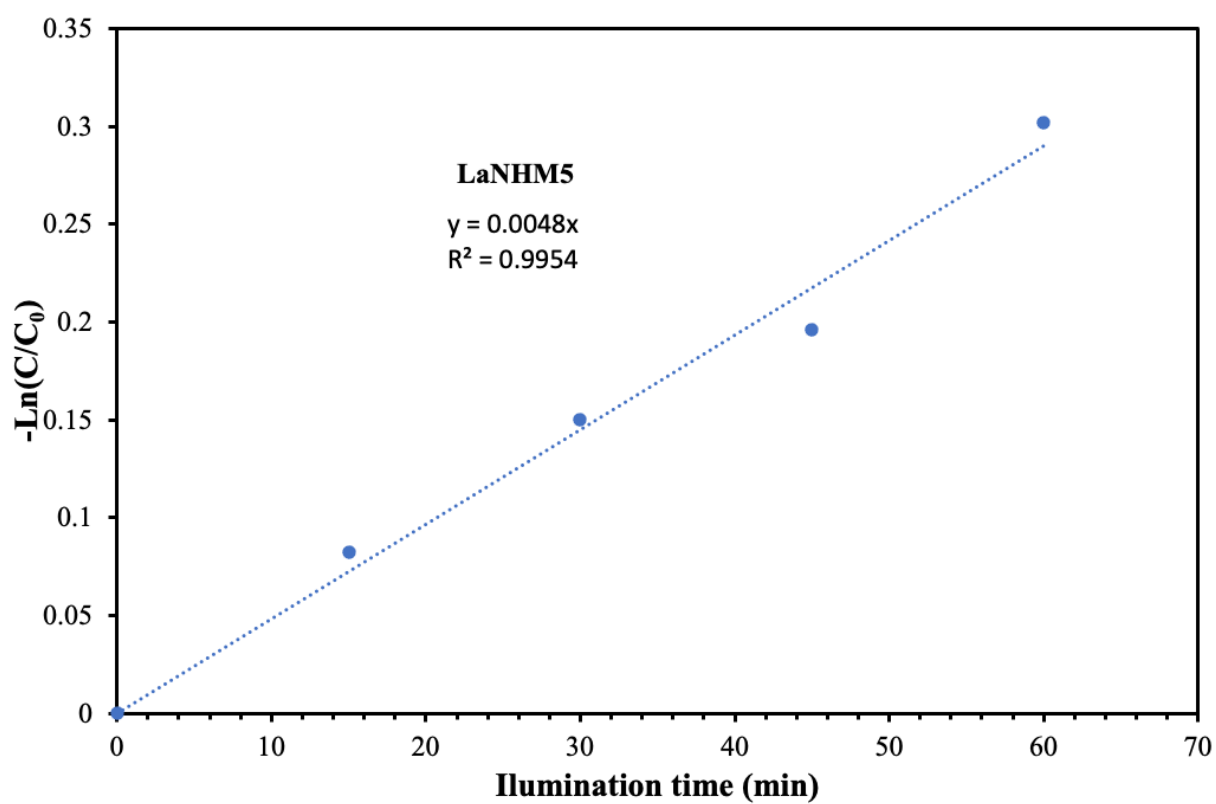
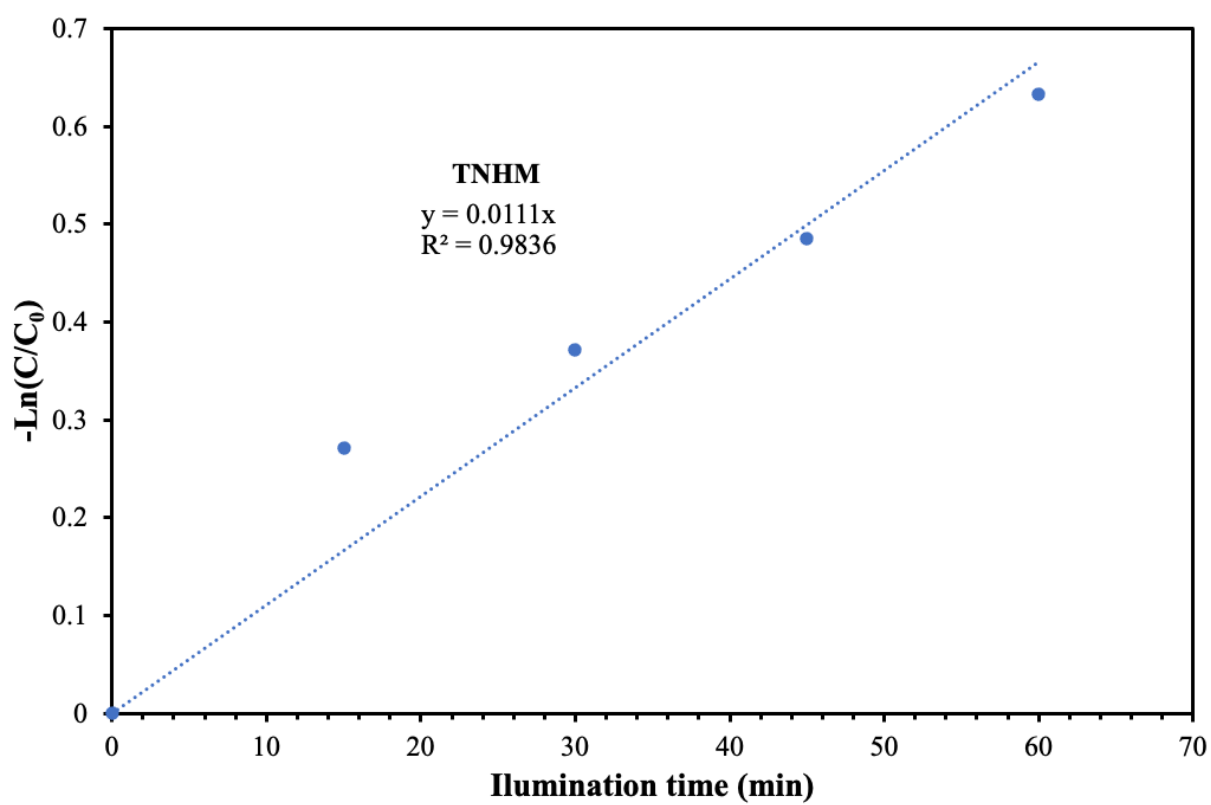
List of Publications

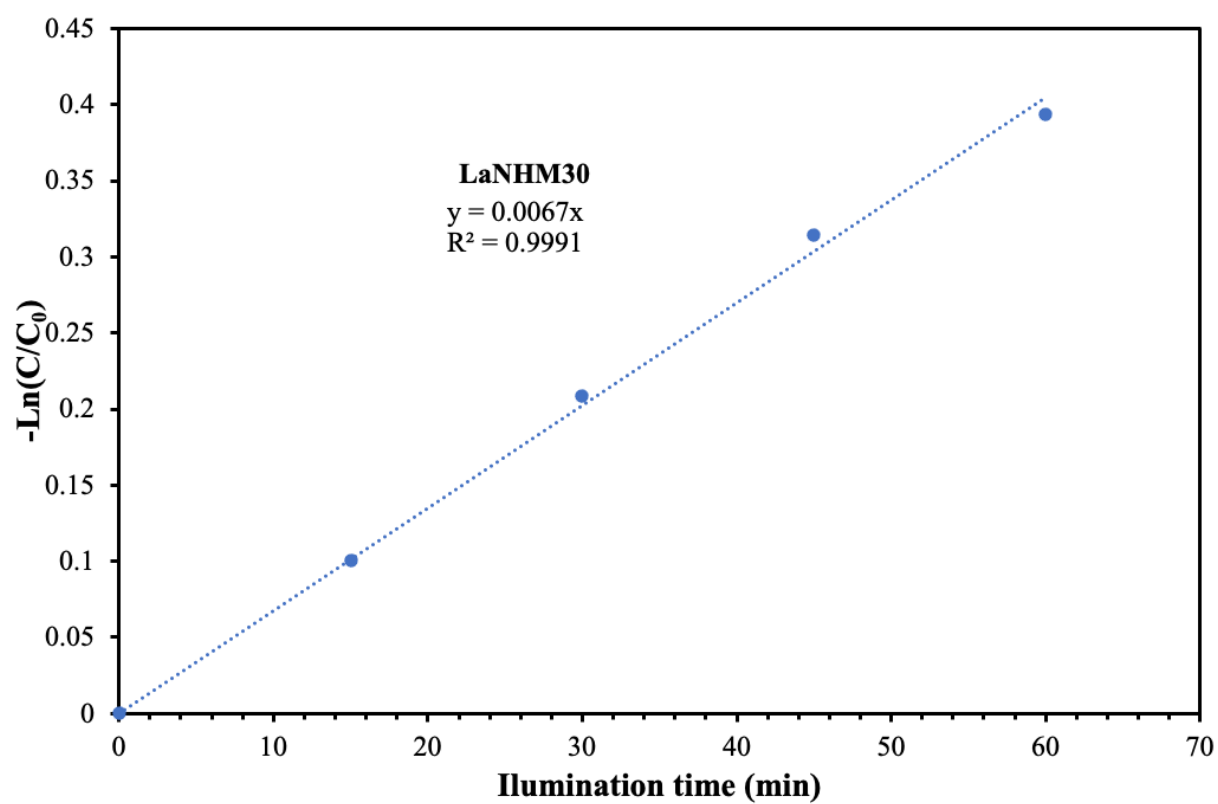
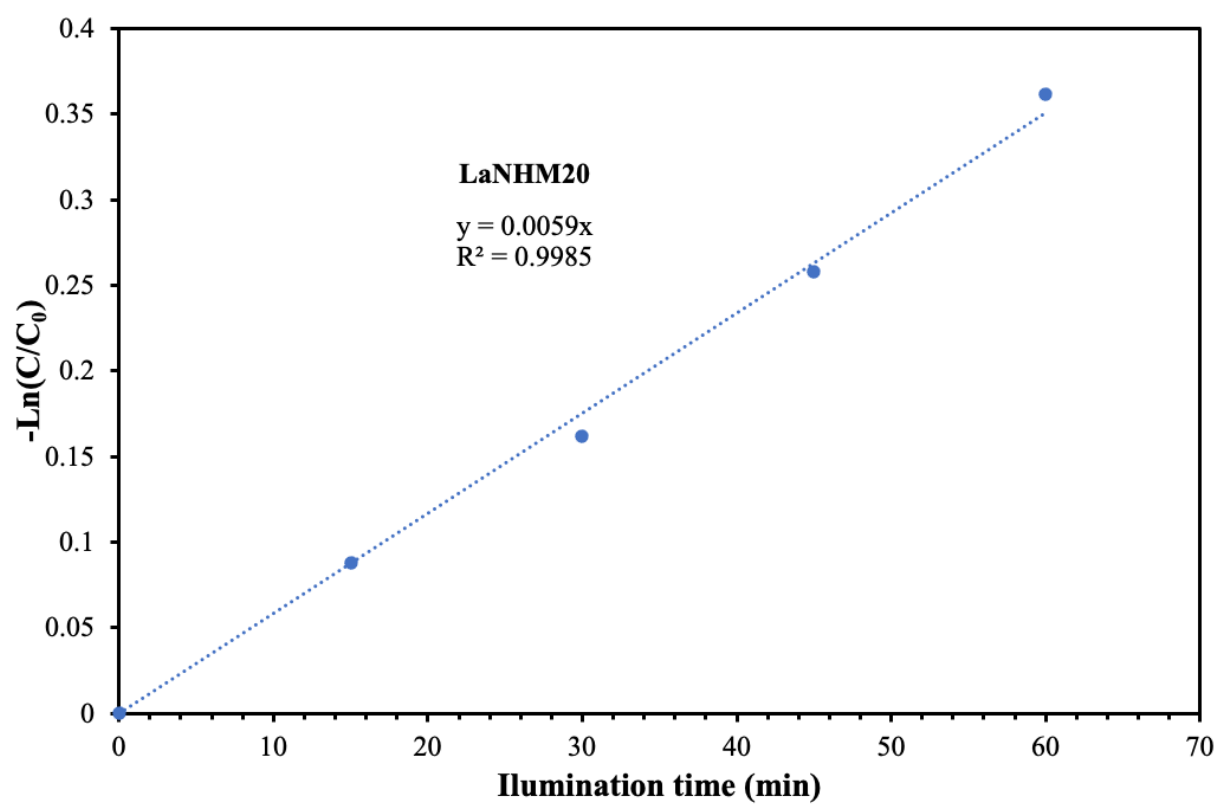
- Tahir, M., Ajiwokewu, B., Bankole, A. A., Ismail, O., Al-Amodi, H., & Kumar, N. (2023). MOF based composites with engineering aspects and morphological developments for photocatalytic CO₂ reduction and hydrogen production: A comprehensive review. *Journal of Environmental Chemical Engineering*, 109408. <https://doi.org/10.1016/j.jece.2023.109408>
- Yusuf, A., Sodiq, A., Giwa, A., Eke, J., Pikuda, O., Eniola, J. O., ... & Bilad, M. R. (2022). Updated review on microplastics in water, their occurrence, detection, measurement, environmental pollution, and the need for regulatory standards. *Environmental Pollution*, 292, 118421. <https://doi.org/10.1016/j.envpol.2021.118421>

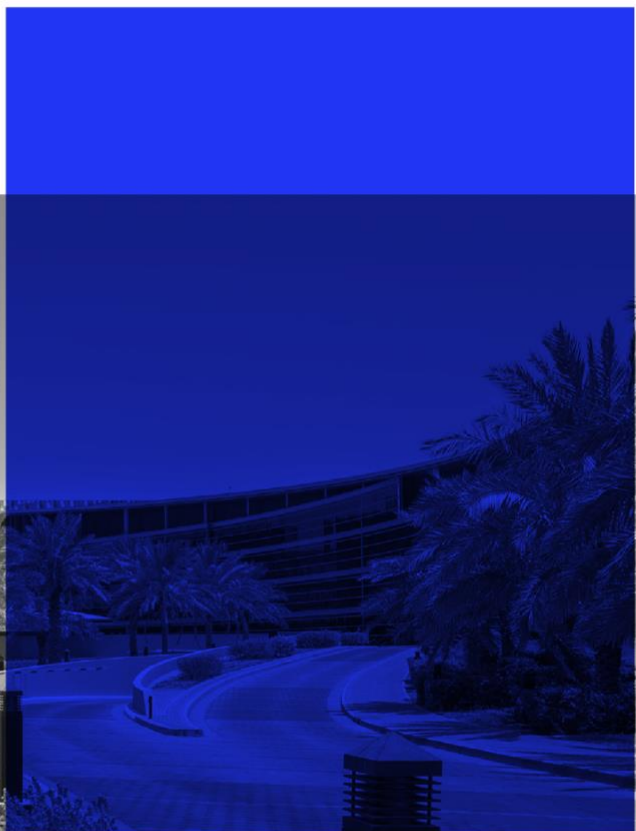
Appendix

Pseudo-first order reaction data for MOF and MOF composites prepared for the photodegradation of CIP under white light irradiation.









UAEU MASTER THESIS NO. 2024: 12

The Thesis is research that focused on the development of $\text{TiO}_2/\text{NH}_2\text{-MIL-125}$ composites for the photocatalytic degradation of antibiotics, in this case using ciprofloxacin as a model compound. It was found that $\text{TiO}_2/\text{NH}_2\text{-MIL-125}$ composite performs better than the individual components, while the addition of La to the composite only decreased its photocatalytic efficiencies.

Bilkis Mojisola Ajiwokewu received her Master of Science in Chemical Engineering from the Department of Chemical and Petroleum Engineering, College of Engineering at UAEU, UAE. She received her Bachelor of Science in Chemical Engineering from the Faculty of Technology, Obafemi Awolowo University, Ile-Ife, Nigeria.

www.uaeu.ac.ae